BJ www.biochemj.org

Biochem. J. (2012) **444**, 343–355 (Printed in Great Britain) doi:10.1042/BJ20120125

Feedback regulation by Atf3 in the endothelin-1-responsive transcriptome of cardiomyocytes: Egr1 is a principal Atf3 target

Alejandro GIRALDO*[1], Oliver P. T. BARRETT†[1], Marcus J. TINDALL*‡, Stephen J. FULLER*, Emre AMIRAK*, Bonhi S. BHATTACHARYA‡, Peter H. SUGDEN* and Angela CLERK*[2]

*Institute of Cardiovascular and Metabolic Research, School of Biological Sciences, University of Reading, Whiteknights, PO Box 218, Reading RG6 6BX, U.K., †Department of Life Sciences, Imperial College London, London SW7 2AZ, U.K., and ‡Department of Mathematics and Statistics, University of Reading, Whiteknights, PO Box 220, Reading RG6 6AX, U.K.

Endothelin-1 promotes cardiomyocyte hypertrophy by inducing changes in gene expression. Immediate early genes including *Atf3* (activating transcription factor 3), *Egr1* (early growth response 1) and *Ptgs2* (prostaglandin-endoperoxide synthase 2) are rapidly and transiently up-regulated by endothelin-1 in cardiomyocytes. Atf3 regulates the expression of downstream genes and is implicated in negative feedback regulation of other immediate early genes. To identify Atf3-regulated genes, we knocked down Atf3 expression in cardiomyocytes exposed to endothelin-1 and used microarrays to interrogate the transcriptomic effects. The expression of 23 mRNAs (including Egr1 and Ptgs2) was enhanced and the expression of 25 mRNAs was inhibited by Atf3 knockdown. Using quantitative PCR, we determined that knockdown of Atf3 had little effect on up-regulation of Egr1 mRNA over 30 min, but abolished the subsequent decline, causing sustained Egr1 mRNA expression and enhanced protein expression. This resulted from direct binding of Atf3 to the Egr1 promoter. Mathematical modelling established that Atf3 can suffice to suppress Egr1 expression. Given the widespread co-regulation of Atf3 with Egr1, we suggest that the Atf3–Egr1 negative feedback loop is of general significance. Loss of Atf3 caused abnormal cardiomyocyte growth, presumably resulting from the dysregulation of target genes. The results of the present study therefore identify Atf3 as a nexus in cardiomyocyte hypertrophy required to facilitate the full and proper growth response.

Key words: activating transcription factor 3 (Atf3), early growth response 1 (Egr1), hypertrophy, immediate early gene, microarray, negative feedback.

INTRODUCTION

Cardiomyocytes, the terminally differentiated contractile cells of the heart, undergo hypertrophy (i.e. increase in cell size) in response to GqPCR (G_q-protein-coupled receptor) agonists including ET-1 (endothelin-1) [1]. ET-1 particularly activates the ERK1/2 (extracellular-signal-regulated kinase 1/2) cascade, a pathway that is associated with cardiomyocyte hypertrophy [1,2]. ERK1/2 signalling is strongly implicated in transcriptional regulation and elicits many longer term effects through changes in gene expression [3]. Perhaps unsurprisingly therefore, ~70 % of the changes in gene expression induced in neonatal rat cardiomyocytes over the first 4 h of stimulation with ET-1 requires ERK1/2 signalling [4–6]. However, activation of ERK1/2 in cardiomyocytes by ET-1 is rapid and transient [7], and this phase may be viewed as an initiating trigger of the longer term response. Consistent with this, exposure of cardiomyocytes to ET-1 results in multiphasic patterns of gene expression that presumably culminate in hypertrophic growth [5]. Our previous studies identified a number of IEGs (immediate early genes; genes that are regulated by pre-existing transcription factors) that are particularly rapidly up-regulated in cardiomyocytes exposed to ET-1 including Atf (activating transcription factor) 3 [5].

Atf3 is a member of the ATF/CREB [CRE (cAMP-response element)-binding protein] family proteins which bind as homo- or hetero-dimers to consensus ATF/CRE sites in gene promoters to regulate transcription [8]. Like other members of this family, full-length Atf3 possesses a bZIP (basic leucine zipper) domain for dimerization, although alternative splicing can produce Atf3 isoforms without a bZIP domain. The activity of some ATF/CREB proteins is regulated by phosphorylation, but Atf3 is largely regulated at the level of expression, being present at very low levels in quiescent cells and induced as an IEG by a range of extracellular stimuli (e.g. peptide growth factors, GqPCR agonists and cytokines) and cellular stresses (e.g. oxidative stress and ischaemia/reperfusion) in a variety of cell types. Indeed, it is difficult to identify a stimulus that does not induce Atf3 expression, suggesting that it plays a significant global role in regulating gene expression programmes. MAPKs (mitogen-activated protein kinases) including ERK1/2 are particularly implicated in promoting *Atf3* mRNA expression, potentially acting through a variety of transcription factors (e.g. CREB, Atf2 and c-Myc) [9–11]. Several studies also implicate the Egr1 (early growth response 1) transcription factor in positive regulation of Atf3 transcription, probably resulting from its phosphorylation and activation by ERK1/2 [10,12,13].

Atf3 is generally viewed as a transcriptional repressor, particularly when present as homodimers. Thus Atf3 represses transcription of Gadd153 (growth arrest and DNA damage-inducible protein 153)/Chop10 [C/EBP (CCAAT/enhancer-binding protein)

Abbreviations used: AdV, adenovirus; Areg, amphiregulin; Atf, activating transcription factor; bZIP, basic leucine zipper; ChIP, chromatin immunoprecipitation; CRE, cAMP-response element; CREB, CRE-binding protein; Dusp, dual specificity phosphatase; Egr1, early growth response 1; ERK1/2, extracellular-signal-regulated kinase 1/2; ET-1, endothelin-1; FDR, false discovery rate; Gapdh, glyceraldehyde-3-phosphate dehydrogenase; GqPCR, G_q-protein-coupled receptor; HEK, human embryonic kidney; IEG, immediate early gene; IL, interleukin; Il1rl1, IL1 receptor-like 1; MAPK, mitogen-activated protein kinase; MOI, multiplicity of infection; NF-κB, nuclear factor κB; qPCR, quantitative PCR; SNK, Student-Newman-Keuls; sqPCR, semi-qPCR; TLR, Toll-like receptor.

[1] These authors contributed equally to this work.
[2] To whom correspondence should be addressed (email a.clerk@reading.ac.uk).

homologous protein 10]/DDIT3 (DNA-damage-inducible transcript 3 protein) and may also repress transcription from its own promoter to limit expression [14]. A systems biology study of TLR (Toll-like receptor) 4 signalling to gene expression in macrophages further confirmed its role as a transcriptional repressor, demonstrating that Atf3 is induced by lipopolysaccharide and represses expression of IL (interleukin) 6 and IL12b mRNAs by antagonizing NF-κB (nuclear factor κB)-dependent stimulation of transcription [15]. A similar system operates downstream from TLR9 [16], suggesting that negative feedback regulation of cytokine production by Atf3 is a feature of the innate immune response [17]. However, Atf3 (potentially as heterodimers with other ATF/CREB proteins) promotes transcription of other genes such as proglucagon [18]. Moreover, in the context of DNA damage in cancer cells, Atf3 may act as a positive regulator of gene expression, probably by enhancing p53 function [19]. The dichotomous role of Atf3 and the variation in underlying mutations that cause cancer presumably account for the variation in opinion regarding the role of Atf3 in this disease [17].

As mentioned above, Atf3 is induced in cardiomyocytes by ET-1 as an IEG [5], but it is also up-regulated in these cells by, for example, doxorubicin [20], oxidative stress [3], insulin [21] and hypoxia [22]. Transient ischaemia increases Atf3 expression in whole hearts [22,23], and cardiospecific overexpression of Atf3 in transgenic mice results in pathological features of cardiac hypertrophy/failure [24] (this is distinguishable from, though may encompass, cardiomyocyte hypertrophy [25]). Confusingly, cardiac hypertrophy/failure induced by pressure overload is exaggerated in Atf3-null mice [26]. This probably results from enhanced signalling through ERK1/2 and other MAPKs, all of which are implicated in the development of cardiac pathology [1]. Although these studies suggest that control of Atf3 expression is important in homoeostatic control of cardiac function, it is difficult to develop a mechanistic understanding of Atf3 function in these models with long-term manipulation of Atf3 expression. We used the cardiomyocyte model to investigate the role of Atf3 in negative feedback regulation of IEG expression and positive feed-forward regulation of second-phase genes. Adopting an antisense knockdown approach, we identified Egr1 as a prime target for Atf3 repression in response to ET-1. Notably, Egr1 has been associated with cardiac hypertrophy for many years [27–29], and the results of the present study shed further light on the transcriptional networks within which it operates.

EXPERIMENTAL

Cardiomyocyte cultures and knockdown of Atf3 with adenoviruses for antisense Atf3

Ventricles from neonatal Sprague–Dawley rat hearts (Harlan) were dissociated by serial digestion and cultured as described previously [6]. For immunoblotting, RNA studies or ChIP (chromatin immunoprecipitation), cardiomyocytes were plated in 15 % (v/v) fetal bovine serum at a density of 4×10^6 cells/dish on 60 mm Primaria dishes pre-coated with sterile 1 % (w/v) gelatin (Sigma–Aldrich). For immunostaining experiments, glass coverslips were placed in Primaria 35 mm culture dishes and coated with 1 % (v/v) gelatin then laminin (0.2 mg/ml in PBS, 2 h). Coverslips were washed with PBS. Cardiomyocytes were plated at 1.5×10^6 cells/dish in serum-containing medium. After 18 h, cardiomyocytes were incubated in serum-free medium for 24 h then unstimulated (controls) or exposed to 100 nM ET-1 (Bachem) in the presence or absence of cycloheximide (Sigma–Aldrich), U0126 or PD184352 (Enzo Life Sciences). Agonists/inhibitors were prepared as 1000× stock solutions in water (ET-1, cycloheximide) or DMSO (U0126, PD184352) and added directly to the tissue culture medium.

Preparation of AdVs (adenoviruses)

Replication-deficient AdVs expressing full-length rat Atf3 antisense RNA (AS-Atf3) were prepared using the AdEasy™ XL Adenoviral Vector System (Stratagene). The coding sequence for Atf3 was isolated by PCR from rat cardiomyocyte cDNA using Pfu polymerase and primers designed to the 5′ start site (5′-ATGATGCTTCAACATCCAGGC-3′) and 3′ stop codon (5′-TTAGCTCTGCAATGTTCCTTC-3′) regions, and further amplified with primers that included sites for restriction enzymes HindIII (5′-CTTATCTAGAAGCTTATGATGCTTCAACATCCAGGC-3′) and KpnI (5′-TAGAGATCTGGTACCTTAGCTCTGCAATGTTCCTTC-3′) for insertion into the multiple cloning site of the pShuttle-CMV vector. Control samples were prepared with empty vector (No-AS). Constructs were sequenced using an ABI 3100 Genetic Analyser. Shuttle plasmids were linearized with PmeI and used to transform BJ5183-AD-1 cells. AdV plasmids from positive recombinants were expanded in XL10Gold cells, linearized with PacI and used to transform HEK (human embryonic kidney)-293 cells. AdVs were amplified through subsequent re-infection of HEK-293 cells and titres were determined using Adeno-X™ Rapid Titer kits (Clontech). For experiments with AdVs, cardiomyocytes were incubated in serum-free medium for 4 h, AdVs were added and the cells incubated for a further 48 h.

Immunoblotting

Cardiomyocytes were washed in ice-cold PBS and nuclear extracts prepared for immunoblotting as described previously [30]. Proteins (20 μg) were separated by SDS/PAGE (10 % or 12 % gels) and transferred electrophoretically on to nitrocellulose membranes. Immunoblotting was performed as described previously [5]. Primary antibodies against Atf3 (sc-188), Egr1 (sc-189) and Atf2 (sc-187) were from Santa Cruz Biotechnology and used at a 1/1000 dilution. Secondary antibodies conjugated to horseradish peroxidase were from Dako (1/5000 dilution). Bands were detected using ECL (enhanced chemiluminescence) Plus with an ImageQuant 350 digital imager (GE Healthcare). ImageQuant 7.0 software was used for densitometric analysis.

RNA preparation, microarrays and data analysis

Cardiomyocytes were uninfected or infected with empty AdVs or AdVs encoding AS-Atf3 and then unstimulated (controls) or exposed to 100 nM ET-1 (90 min). Uninfected cardiomyocytes were exposed to ET-1 for 30, 60 or 90 min. Total RNA was prepared and concentrations determined as described previously [5]. To minimize the variation resulting from different cardiomyocyte preparations, equal amounts of RNA from three individual experiments were pooled to generate a single sample set. A total of three sets of pooled samples were prepared for hybridization to separate Affymetrix rat exon 1.0 ST arrays (i.e. three separate sets of samples were analysed for each condition, prepared from a total of nine myocyte preparations). Samples were prepared for hybridization using Genechip® WT Sense Target Labelling kits (Affymetrix). For all samples, except those from uninfected cells exposed to ET-1 for 60 min with their corresponding controls, the rRNA reduction protocol was modified and the RiboMinus Transcriptome Isolation Kit (Human/Mouse) (Invitrogen) was used according to the manufacturer's instructions with 7 μg of RNA. Hybridization to

Affymetrix rat exon 1.0 ST arrays was performed at the CSC/IC Microarray Centre (Imperial College London, London, U.K.). For samples from uninfected cells exposed to ET-1 for 60 min with their corresponding controls, total RNA was provided to the European *Arabidopsis* Stock Centre at Nottingham (NASC) for preparation and hybridization to Affymetrix rat exon 1.0 arrays according to their protocols (http://affymetrix.arabidopsis.info). The results are available from ArrayExpress (accession numbers E-MEXP-3392, E-MEXP-3393 and E-MEXP-3394).

The data (.CEL files) were imported into GeneSpring 11.5 (Agilent Technologies) using the Extended annotations, with RMA16 normalization and normalization per gene to corresponding uninfected unstimulated controls within each sample set. Probesets were selected for analysis with baseline expression >50 in all of any of the conditions. To determine effects of AdV infection, probesets were selected with >1.5-fold change in unstimulated cells infected with No-AS AdVs relative to uninfected cells, applying an unpaired Student's t test with the Benjamini and Hochberg multiple testing correction [FDR (false discovery rate)<0.05)]. To identify transcripts regulated by Atf3, we selected those which were significantly changed (>1.5-fold; FDR<0.05) in uninfected cells in response to ET-1 at 30, 60 or 90 min (unpaired Student's t tests with the Benjamini and Hochberg multiple testing correction). For transcripts with <1.2-fold change in baseline expression with No-AS AdVs, subsequent analysis employed an interpretation with AdV-infected conditions, using statistical testing [one-way ANOVA with SNK (Student-Newman-Keuls) post-test and Benjamini and Hochberg multiple testing correction] and filtering on the basis of >1.5-fold difference between AS-Atf3 and No-AS infected cells. For transcripts with >1.2-fold change in baseline expression with No-AS AdVs, subsequent analysis employed an interpretation with all conditions, using statistical testing (one-way ANOVA with SNK post-test and the Benjamini and Hochberg multiple testing correction) to identify mRNAs with significant difference between cells infected with AS-Atf3 and No-AS AdVs or uninfected cells, but with no significant difference between uninfected cells and those infected with No-AS AdVs with exposure to ET-1 (90 min) and/or in unstimulated cells. Further filtering identified transcripts with >1.5-fold difference between cells infected with AS-Atf3 and those infected with No-AS AdVs or uninfected cells.

PCR

Cardiomyocytes were treated and total RNA extracted as for microarray analysis. cDNAs were synthesized using High Capacity cDNA Reverse Transcription Kits with random primers (Applied Biosystems). sqPCR [semi-qPCR (quantitative PCR)] and qPCR were performed as described previously [5] using primers listed in Supplementary Table S2 (at http://www.BiochemJ.org/bj/444/bj4440343add.htm). Values were normalized to Gapdh (glyceraldehyde-3-phosphate dehydrogenase) expression and then to control values.

ChIP

Cardiomyocytes (16×10^6 cells per sample) were unstimulated or exposed to 100 nM ET-1 and fixed in 1 % (v/v) formaldehyde (10 min). The reaction was terminated with 125 mM glycine (10 min). Cells were washed and harvested in ice-cold PBS containing protease/phosphatase inhibitors [5], collected by centrifugation (3000 ***g*** at 4 °C for 5 min) and lysed (15 min at 4 °C) in 50 mM Tris/HCl (pH 8.0), 2 mM EDTA, 0.1 % Nonidet P40 and 10 % (v/v) glycerol containing protease/phosphatase inhibitors. Nuclei were pelleted (3000 ***g*** at 4 °C for 5 min), resuspended in 50 mM Tris/HCl (pH 8.0), 1 % (w/v) SDS and 5 mM EDTA, and the DNA sheared to 200–800 bp fragments by sonication (5×30 s with 2 min recovery at 4 °C). Following centrifugation (4000 ***g*** at 4 °C for 5 min), the supernatants were retained and a sample reserved for input DNA. The remainder was diluted in 50 mM Tris/HCl (pH 8.0), 0.5 % Nonidet P40, 200 mM NaCl and 0.5 mM EDTA. Samples were pre-cleared with Protein A–Sepharose then incubated without or with 0.01 mg of anti-Atf3 antibodies (Santa Cruz Biotechnology, catalogue number sc-188X) with rotation (overnight at 4 °C). Protein A–Sepharose was added together with sonicated salmon sperm DNA (1 μg/ml) and samples were incubated (4 °C for 2 h). Beads were pelleted by centrifugation (1000 ***g*** at 4 °C for 3 min) and washed (4 °C for 3 min) in 20 mM Tris/HCl (pH 8.0), 0.1 % SDS, 1 % (v/v) Nonidet P40, 2 mM EDTA and 500 mM NaCl followed by 10 mM Tris/HCl (pH 8.0) containing 1 mM EDTA. Immune complexes were eluted (10 min at 65 °C) in 10 mM Tris/HCl (pH 8.0), 1 mM EDTA and 1 % (w/v) SDS. Samples were centrifuged (200 ***g*** for 1 min) and the supernatants collected. Cross-links were reversed by incubation (overnight at 65 °C) with 0.2 M NaCl. Samples were incubated (5 min at 4 °C) with phenol/chloroform/3-methylbutan-1-ol (25:24:1, pH 8.0) and the phases separated by centrifugation (15 300 ***g*** at 4 °C for 10 min). DNA in the upper aqueous phase was precipitated with isopropanol (-80 °C for 3 h), recovered by centrifugation (15 300 ***g*** for 10 min at 4 °C), washed [70 % (v/v) ethanol] and resuspended in nuclease-free water for PCR. PCR reactions were performed using specific primers: Egr1 forward, 5′-ACTGCCGCTGTTCCAATACT-3′; Egr1 reverse, 5′-CGAATCGGCCTCTATTTCAA-3′; Ptgs2 forward, 5′-GCAGCAAGCACGTCAGACT-3′; Ptgs2 reverse, 5′-TAACCCGGAGAACCTTGCTT-3′; IL6 forward, 5′-TGCTCA-AGTGCTGAGTCACT-3′; IL6 reverse, 5′-AGACTCATGG-GAAAATCCCA-3′. The primers for an arbitrary downstream sequence ~2000 bp 3′ to the IL6 promoter were: forward, 5′-CACCTCTCCACCCTGACATT-3′ and reverse, 5′-CCAACTAGACAGCCCAGAGC-3′. PCR amplification conditions were: 34 cycles of denaturing at 95 °C for 30 s, annealing at 60 °C for 30 s and extension at 72 °C for 45 s. PCR products were visualized on 2 % (w/v) agarose gels with Sybr-Safe (Invitrogen) and the bands captured under UV illumination. Densitometric analysis was performed using Imagemaster 1D Prime, version 3.0 (GE Healthcare).

Immunostaining

Cardiomyocytes were exposed to 100 nM ET-1, then washed with PBS and fixed in 4 % (v/v) formaldehyde [10 min at room temperature (25 °C)]. Immunostaining was performed as described previously [31] using mouse monoclonal primary antibodies against troponin T (1/40 dilution for 60 min; Stratech Scientific, catalogue number MS-295-P1) and Alexa Fluor® 488 anti-mouse secondary antibodies (1/200 dilution for 60 min). Coverslips were mounted using fluorescent mounting medium (Dako) and viewed using a Zeiss Axioskop fluorescence microscope. Images were captured using a digital camera (1600×1200 pixels resolution, $\times1.4$ zoom factor and 160×120 μm field dimension). Colour images were converted to greyscale using Adobe Photoshop.

Statistical analysis

Statistical analysis of microarray data used GeneSpring 11.5. Other analyses used GraphPad Prism 4.0.

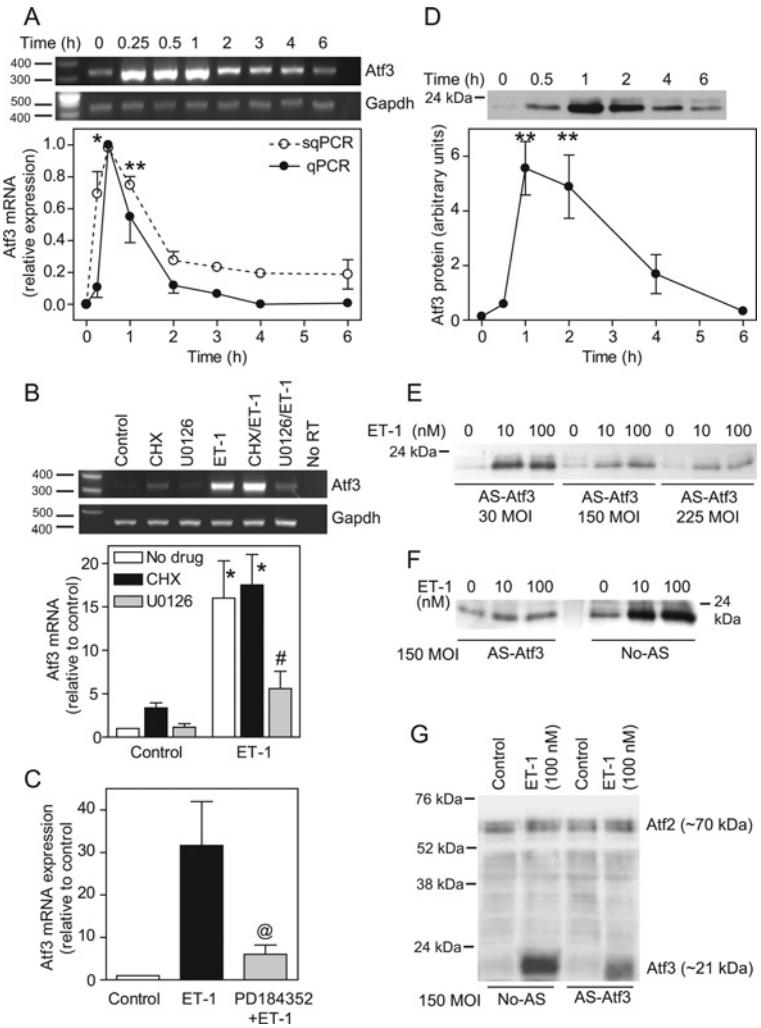

Figure 1 ***Atf3*** **mRNA and protein is increased in cardiomyocytes exposed to ET-1 and suppressed by AS-Atf3**

Cardiomyocytes were unstimulated (control) or exposed to 100 nM ET-1 for the times indicated (**A**), were exposed for 0.5 h to 20 μM cycloheximide (CHX), or 10 μM U0126, ET-1, or ET-1 in the presence of CHX or U0126 (**B**) or were exposed to ET-1 in the absence or presence of 2 μM PD184352 (**C**). RNA was extracted and *Atf3* mRNA expression measured by sqPCR (**A** and **B**) or qPCR (**A** and **C**). For (**A**) and (**B**) the representative sqPCR images are for Atf3 (upper image, 388 bp amplicon) and Gapdh (lower image, 412 bp amplicon). Positions of markers are shown on the left-hand side and controls with no reverse transcriptase (RT) were negative. Densitometric analysis for sqPCR of Atf3 is shown in the lower panels. In (**A**) sqPCR and qPCR data are compared and results are a range from 0 (control values) to 1 (maximal expression at 0.5 h). All data were normalized to Gapdh and are means $\pm$ S.E.M. for three or four myocyte preparations. (**D**) Cardiomyocytes were exposed to ET-1 for the times indicated and nuclear extracts (20 μg of protein) immunoblotted with antibodies against Atf3 using 12 % polyacrylamide gels. Atf3 was detected as a band of $\sim$ 21 kDa. A representative image is shown (upper panel) with densitometric analysis (lower panel). Results are mean $\pm$ S.E.M. for three myocyte preparations. (**E**–**G**) Cardiomyocytes were infected with No-AS or AS-Atf3 AdVs at the indicated MOI and unstimulated (control) or stimulated with 0, 10 or 100 nM ET-1. Nuclear extracts were immunoblotted for Atf3 using 12 % (**E** and **F**) or 10 % (**G**) polyacrylamide gels. In (**G**) the blots were divided into upper and lower sections and were probed with antibodies against Atf2 and Atf3 respectively. Atf2 was detected at $\sim$ 70 kDa. @$P < 0.05$ relative to ET-1; *$P < 0.001$ relative to control; **$P < 0.01$ relative to control; #$P < 0.001$ relative to ET-1 (one way ANOVA with SNK post-test). In all of the gels, the positions of relative molecular mass markers are given in kDa on the left-hand side.

RESULTS

Regulation of Atf3 expression in cardiomyocytes by ET-1 and identification of Atf3 target genes

ET-1 (100 nM) stimulated a rapid transient increase in expression of Atf3 mRNA in cardiomyocytes (Figure 1A). Expression was maximal within 30 min, declining rapidly thereafter. Cycloheximide (a protein synthesis inhibitor) did not inhibit the response, indicating that Atf3 was regulated as an IEG (Figure 1B), and up-regulation of Atf3 mRNA by ET-1 was inhibited by U0126 or PD184352, inhibitors of the ERK1/2 cascade (Figures 1B and 1C). Atf3 protein was also increased by ET-1 (maximal at 1 h) (Figure 1D). To suppress expression of Atf3, we generated AdVs encoding full-length Atf3 in the antisense orientation (AS-Atf3), using empty AdVs with no AS-Atf3 (No-AS) to control for effects of viral infection. Effective knockdown of Atf3 protein induced by ET-1 was obtained using 150 MOI (multiplicity of infection) AS-Atf3 AdVs with limited effect of No-AS AdVs and no effect on expression of Atf2 (Figures 1E–1G).

Uninfected cardiomyocytes or cardiomyocytes infected with 150 MOI No-AS or AS-Atf3 AdVs were unstimulated or exposed to 100 nM ET-1 for 90 min (since expression of Atf3 protein was maximal at 1 h, we expected to detect downstream consequences by 90 min; Figure 1D) and mRNA expression profiling was performed (Affymetrix rat exon 1.0 ST microarrays). As expected, No-AS AdV infection alone significantly (>1.5-fold; FDR<0.05)

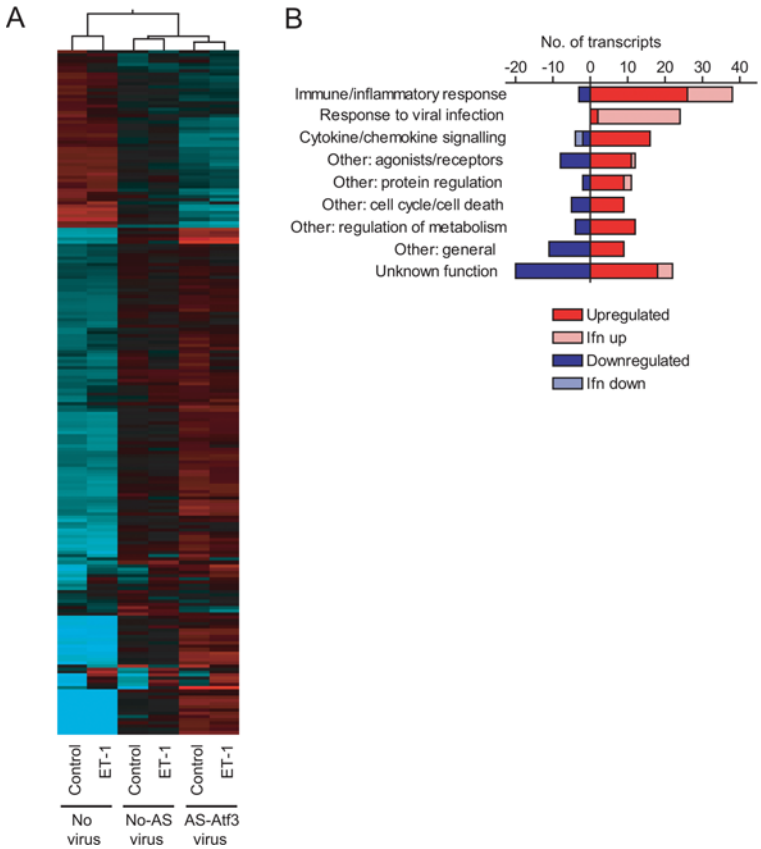

Figure 2 Infection with AdVs modulates expression of a subset of cardiomyocyte mRNAs

Cells (uninfected or infected with 150 MOI No-As or AS-Atf3) were unstimulated or exposed to ET-1 for 90 min and RNA expression profiles determined using Affymetrix rat exon 1.0 ST arrays. (**A**) Heatmaps show expression profiles for probesets that were significantly changed (>1.5-fold, FDR < 0.05) by viral infection alone. Normalization is to the gene median [range is -2.5 (cyan) through 0 (black) to $+2.5$ (red) on a $\log_2$ scale]. Results are means for three hybridizations each representing three independent myocyte preparations. Clustering on conditions and entities used a Euclidean distance matrix and centroid linkage ratio. (**B**) Transcripts were classified according to function. Up- and down-regulated transcripts are in red and blue respectively. Transcripts regulated by interferons (Ifn) in other systems are in lighter colours.

affected expression of a subset of mRNAs (156 mRNAs up-regulated and 59 mRNAs down-regulated), many of which are associated with a viral response and/or cytokine/chemokine signalling in other cells (Figure 2 and Supplementary Table S3 at http://www.BiochemJ.org/bj/444/bj4440343add.htm).

To determine the effects of Atf3 in the ET-1-responsive myocyte transcriptome, probesets were selected with significant changes in expression (>1.5-fold, FDR<0.05) induced by ET-1 at 30, 60 or 90 min (334 up-regulated and 109 down-regulated mRNAs). From these, we identified 90 mRNAs that were up-regulated by ET-1 and affected by Atf3 knockdown (Figure 3A and Supplementary Tables S4–S6 at http://www.BiochemJ.org/bj/444/bj4440343add.htm). Of the up-regulated transcripts without a baseline effect of viral infection (75 mRNAs), AS-Atf3 enhanced the response of 15 mRNAs (clusters A1 and A2), inhibited the response of 18 mRNAs (clusters B1 and B2) and, for 42 mRNAs (cluster C), AS-Atf3 enhanced the response in unstimulated cells without further effect on the response to ET-1. Of the up-regulated mRNAs with a baseline effect (>1.2-fold change) of viral infection, the response to ET-1 was enhanced or inhibited by AS-Atf3 for eight (cluster D) or seven (cluster E) mRNAs respectively. With ET-1-down-regulated mRNAs (Figure 3B and Supplementary Table S7 at http://www.BiochemJ.org/bj/444/bj4440343add.htm), we identified only five mRNAs for which AS-Atf3 reduced the magnitude of the down-regulation by ET-1 (cluster F) and five mRNAs for which AS-Atf3 increased the magnitude of the response (cluster G). Having previously defined IEGs compared with downstream gene expression for mRNAs up-regulated by ET-1 (Affymetrix rat genome 230 2.0 arrays) [5], we cross-referenced the datasets (Supplementary Tables S4 and S6). A greater proportion of mRNAs in clusters A1, A2 and D (Atf3-knockdown-enhanced ET-1-induced expression) were IEGs rather than second-phase genes, consistent with negative feedback by Atf3. A greater proportion of mRNAs in clusters B1 and B2 (Atf3-knockdown-inhibited ET-1-induced expression) were second-phase genes rather than IEGs, suggesting that Atf3 plays a positive feed-forward role in these cases (genes in cluster E were not identified in the previous dataset [5]). Overall, we conclude that up-regulation of Atf3 by ET-1 in cardiomyocytes plays a significant role in modulating the response of other up-regulated genes and a minor role in regulating mRNAs that are down-regulated by ET-1.

Negative regulation of *Egr1* and *Ptgs2* expression by Atf3

Microarray data were validated by qPCR, selecting IEGs with enhanced expression of the ET-1 response by AS-Atf3 (*Egr1*

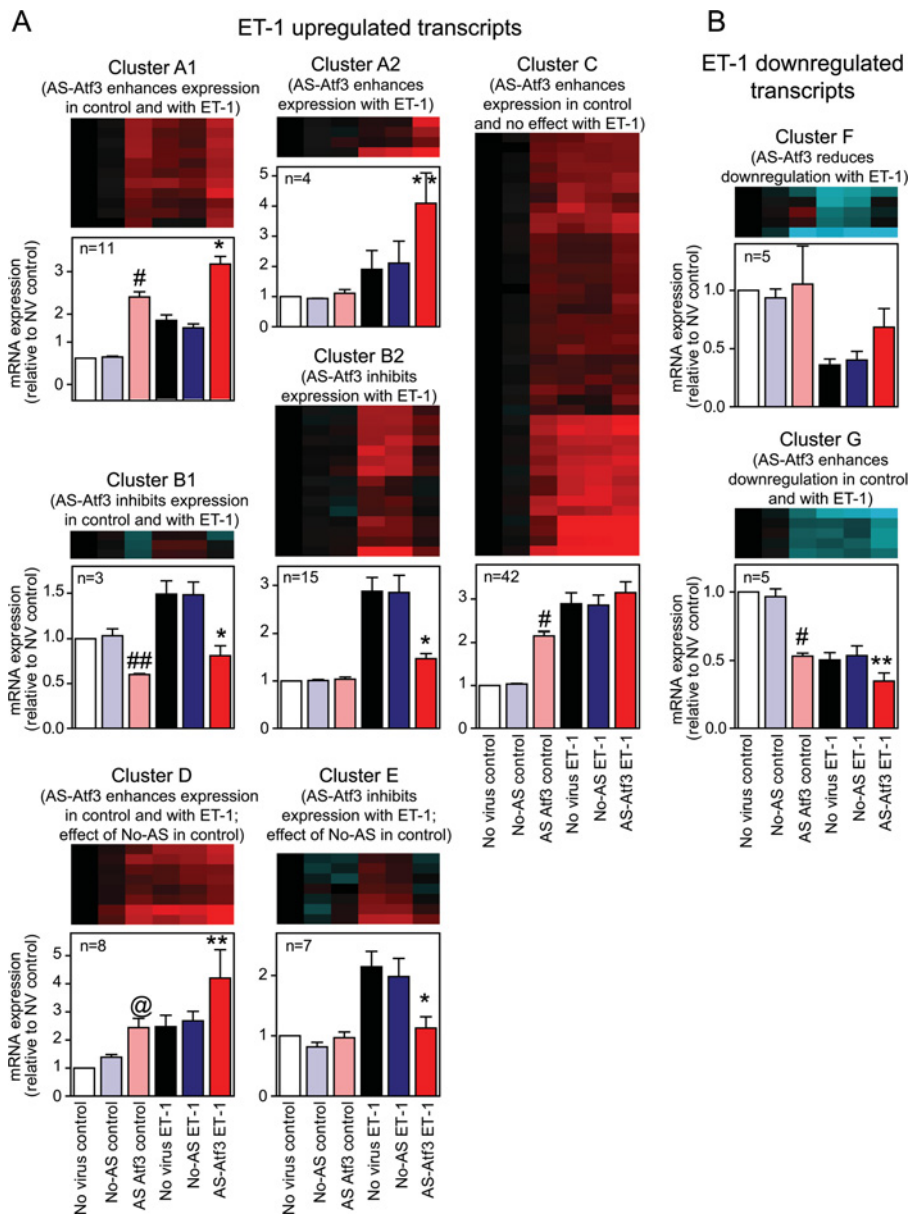

Figure 3 Atf3 knockdown modulates the response of the cardiomyocyte transcriptome to ET-1

Cardiomyocytes were uninfected or infected with No-AS or AS-Atf3 AdVs (150 MOI), then were unstimulated (control) or exposed to ET-1 (100 nM for 90 min). RNA was extracted and analysed using Affymetrix rat exon 1.0 ST arrays. Analysis of transcripts that were up- (**A**) or down-regulated (**B**) by ET-1 identified mRNAs that were significantly changed (>1.5-fold, FDR<0.05) by AS-Atf3 compared with No-AS or uninfected cells in the absence (clusters, A, B, C and F) or presence (clusters D, E and G) of a statistically significant baseline effect (>1.2-fold) of viral infection as determined by GeneSpring analysis ($P < 0.05$). mRNAs were clustered as indicated. Heatmaps are shown for each cluster with normalization to uninfected controls [range is -2.5 (cyan) through 0 (black) to $+2.5$ (red) on a $\log_2$ scale]. Results are means for three hybridizations each representing three independent myocyte preparations. Clustering on entities used a Euclidean distance matrix and centroid linkage ratio. Histograms are means $\pm$ S.E.M. for the relative mRNA expression for each cluster. Each cluster was subjected to further statistical analysis independently of the global-GeneSpring analysis. *$P < 0.001$ relative to No-AS ET-1; **$P < 0.05$ relative to No-AS ET-1; #$P < 0.001$ relative to No-AS control; ##$P < 0.05$ relative to No-AS control; @$P < 0.05$ relative to no virus control (one-way ANOVA with SNK post-test). Although the No-AS effect in control cells is significant in the context of global statistical testing of microarray data, with the small numbers of genes in clusters D and E (with the variation in expression levels) this was not significant with secondary testing. Similarly, for cluster D, although the AS–Atf3 control data are significantly different from the no-virus control, they are not statistically significantly different from the No-AS control.

and *Ptgs2*) and non-IEGs with reduced expression by AS-Atf3 [*Areg* (amphiregulin) and *Dusp* (dual specificity phosphatase) *5*] for analysis. For *Egr1* and *Ptgs2*, the relative increase in expression induced by ET-1 at 0.5 h was similar in cardiomyocytes expressing No-AS or AS-Atf3 (Figures 4A and 4B), indicating that Atf3 was not involved in this up-regulation phase. AS-Atf3 produced sustained expression of *Egr1* mRNA (Figure 4A) and enhanced expression of *Ptgs2* at subsequent times (Figure 4B), consistent with negative feedback of Atf3 on these two genes. In contrast, AS-Atf3 inhibited expression of *Areg* (Figure 4C) and *Dusp5* (Figure 4D). The qPCR data (Figure 4, left-hand panels) are consistent with the microarray results (Figure 4, right-hand panels). *Dusp1* (an IEG) and *Il1rl1* (IL1 receptor-like 1; a non-IEG) were not significantly affected by AS-Atf3 in our microarray experiments and there was no difference in the relative changes in expression induced by ET-1 in cardiomyocytes expressing

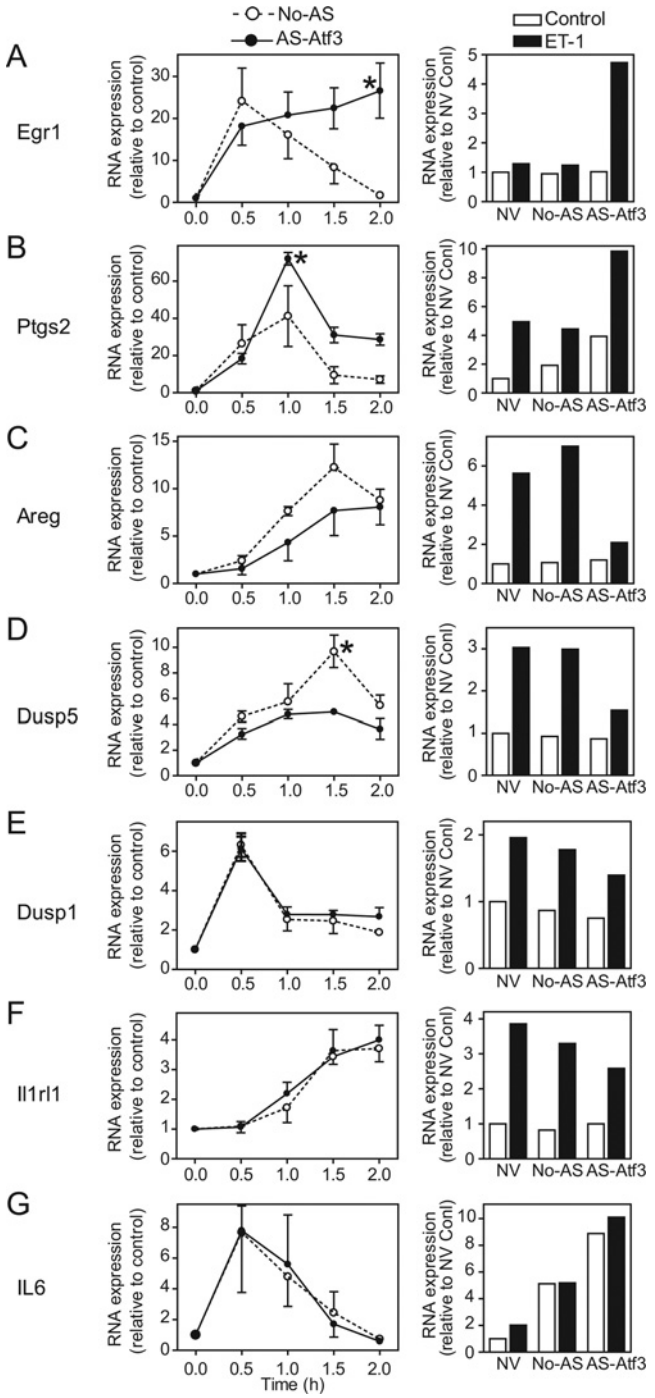

Figure 4 qPCR validation of microarray data

Results were validated for *Egr1* (**A**), *Ptgs2* (**B**), *Areg* (**C**), *Dusp5* (**D**), *Dusp1* (**E**), *Il1rl1* (**F**) and *IL6* (**G**). Left-hand panels: cardiomyocytes were infected with No-AS (○ and broken line) or AS-Atf3 (● and solid line) AdVs, then exposed to 100 nM ET-1 for the times indicated. RNA was extracted and expression of mRNAs analysed by qPCR. Results are means ± S.E.M. for three myocyte preparations. $*P < 0.05$ for AS-Atf3 relative to No-AS at the same time point (one-way ANOVA with SNK post-test). Right-hand panels: microarray data for each of the mRNAs studied are presented relative to uninfected (NV) controls. Results are shown for unstimulated cells (open bars) and cardiomyocytes exposed to ET-1 for 90 min (filled bars). Results are means for three independent myocyte preparations and hybridizations.

No-AS or AS-Atf3 (Figures 4E and 4F). Thus our selection criteria were not excessively stringent. Finally, although others have identified IL6 as a target for negative feedback by Atf3 in the context of inflammation [15], there was no difference in relative expression of *IL6* mRNA in cardiomyocytes expressing No-AS or AS-Atf3 following stimulation with ET-1 at any time studied (Figure 4G). To validate the Atf3–Egr1 feedback loop further, we examined the effect of AS-Atf3 on Egr1 protein expression following induction with ET-1. AS-Atf3 (but not No-AS) inhibited expression of Atf3 for the 150 min period studied (Figures 5A and 5B). AS-Atf3 did not substantially increase the total amount of Egr1 protein at 60 min, but levels remained elevated up to ∼105 min (Figures 5A and 5C). After this time Egr1 protein declined, but levels remained elevated up to at least 150 min.

ChIP with antibodies against Atf3 was used to determine if Atf3 binds directly to the Egr1 and Ptgs2 promoters. The Egr1 promoter contains two CRE elements [32], and a CRE element potentially subject to negative regulation by Atf3 has been identified in the Ptgs2 promoter [33,34]. We used primers either side of these sequences for ChIP–PCR (Figures 6A and 6C). For both genes, the amount of ChIP–PCR product in unstimulated cells was similar to that of the no-antibody controls and stimulation with ET-1 (1 h) substantially increased the amount of ChIP–PCR product (Figures 6B and 6D). Thus Atf3 binds directly to Egr1 and Ptgs2 promoters to inhibit transcription. Interestingly, ChIP–PCR for the IL6 promoter (Figure 6E) demonstrated binding of Atf3 (Figure 6F) despite there being no effect of Atf3 knockdown on expression of IL6 mRNA (Figure 4G). This is discussed below, but potentially results from ET-1 signalling through ERK1/2 rather than NF-κB. The specificity of the ChIP–PCR experiments was demonstrated by PCR across an arbitrary sequence approximately 2000 bp downstream of the IL6 promoter (Figure 6G).

Mathematical modelling of the Atf3–Egr1 negative feedback loop

Atf3 appears to be a dominant-negative regulatory factor in suppressing Egr1 transcription (Figure 4A), but we cannot eliminate the possibility of additional negative regulatory elements from the experimental data. We therefore developed a deterministic ordinary differential equation model for the Atf3–Egr1 feedback system (Figure 7A) to determine whether Atf3 expression can suffice to suppress *Egr1* transcription. We assumed the following: Atf3 and Egr1 are co-regulated through ERK1/2 signalling (expression of each requires a similar degree of ERK1/2 signalling [5]); ERK1/2 promote expression by increasing transactivating activities of transcription factors pre-bound to both promoters (i.e. the transcription factor/promoter is viewed as a single entity regulated by ERK1/2 binding/phosphorylation); and it was not necessary to consider ERK1/2 or Atf3 signal termination (i.e. no attempt was made to switch off the signal). The model was informed initially by parameters derived in the present study and from previously published literature (see the Supplementary Online Data at http://www.BiochemJ.org/bj/444/bj4440343add.htm).

We initially assumed that Atf3 suppression of *Egr1* mRNA transcription was competitive with the positive ERK1/2 signal, but this did not give a good fit with the experimental data. An alternative model in which Atf3 eliminates the ERK1/2 signal (modelled by removing the ERK1/2 signal upon Atf3 binding; Figure 7A) gave a good qualitative fit. Adjusting the rate of mRNA synthesis to 275 bases/s (within the recently estimated range of 55 to >800 bases/s [35,36]) for calculation of the rates of transcription of *Egr1* and *Atf3* mRNAs, and adjusting parameters for association of phosphorylated ERK1/2 with *Egr1* and *Atf3* DNA (see the Supplementary Online Data) gave a very good fit to the experimental data in terms of magnitude of variation in *Egr1* mRNA (∼20-fold; Figure 4A), and a relatively good fit (qualitatively) to the suppression of Egr1 mRNA by Atf3. The

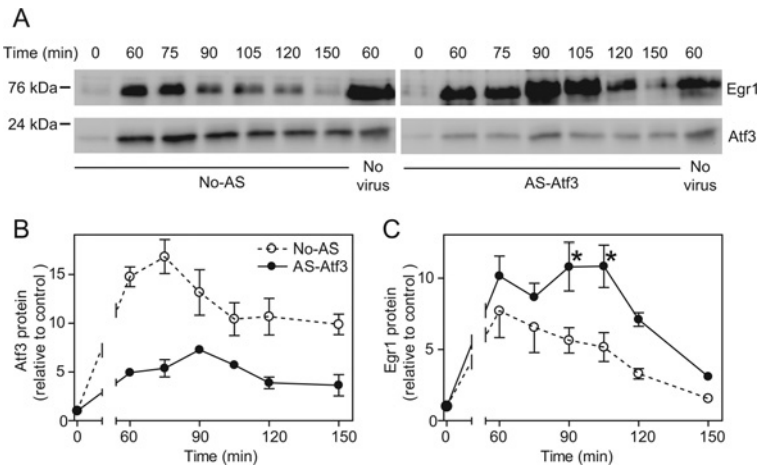

Figure 5 AS-Atf3 expression enhances expression of Egr1 protein in cardiomyocytes exposed to ET-1

Cardiomyocytes were uninfected or were infected with No-AS (○ and broken line) or AS-Atf3 (● and solid line) AdVs, then exposed to 100 nM ET-1 for the times indicated. (**A**) Nuclear extracts (20 μg of protein) were immunoblotted for Egr1 (upper images) or Atf3 (lower images). Representative blots of the same nuclear extracts are shown. Positions of relative molecular mass markers are given in kDa on the left-hand side. (**B**) Densitometric data for expression of Atf3 protein. (**C**) Densitometric data for expression of Egr1 protein. Results were normalized to the no-virus samples on each blot and are means $\pm$ S.E.M. for three myocyte preparations. $^*P < 0.05$ for AS-Atf3 relative to No-AS at the same time point (one-way ANOVA with SNK post-test).

best-fit model was obtained with a rate of Atf3 suppression of Egr1 transcription (k_7) in the range $1\times10^5(Ms)^{-1} \leqslant k_7 \leqslant 6\times10^5(Ms)^{-1}$ (Figure 7B). Modelling the system in the absence of Atf3 (to mimic Atf3 knockdown) resulted in a similar rate of production of *Egr1* mRNA to $\sim$0.5 h, with sustained expression thereafter (Figure 7B, centre left-hand panel), a profile that replicates the experimental data (Figure 4A, left-hand panel). Thus Atf3 alone can account for the suppression of *Egr1* mRNA expression and probably does so by over-riding the positive ERK1/2 signal.

Effects of Atf3 on morphological changes induced in cardiomyocytes by ET-1

To determine the consequences of knockdown of Atf3 for ET-1-induced hypertrophy, we examined the effects of AS-Atf3 AdVs on myocyte morphology by immunostaining for troponin T, a component of the myofibrillar apparatus. As shown previously [37,38], uninfected and unstimulated cardiomyocytes appear small with disorganized myofilaments (Figure 8A). Stimulation with ET-1 increased cell size, increased the content/organization of myofilaments and promoted formation of cell–cell contacts (Figure 8B), classic features of hypertrophy. No-AS AdVs increased myofibrillar content to a small degree in unstimulated cells (Figure 8C), but had no overt effect on morphological changes induced by ET-1 (Figure 8D). Relative to No-AS AdVs, AS-Atf3 AdVs had no effect on unstimulated cells, but resulted in abnormal morphology following ET-1 stimulation with 'clumping' of cells and generation of elongated processes extending between them (Figures 8E–8H). It is unclear if this is an effect on hypertrophy itself or whether there is a loss of cell–cell or cell–matrix adhesion. Thus, although Atf3 is transiently up-regulated within the first hour of stimulation, it has a significant effect on long-term phenotypic changes.

DISCUSSION

Atf3 is emerging as an extremely important feedback regulator of transcription in general. Greatest emphasis has been placed on its role in inflammation and it is clear that Atf3 is essential for restraining the immune response [15,17]. However, although viewed as a stress-regulated and -regulatory gene, *Atf3* is also up-regulated in many cells by growth stimuli including peptide growth factors and GqPCR agonists [5,39–41]. The genes that Atf3 regulates in a growth context are likely to differ from those that it regulates in a stress response. In the present study, we identified a number of genes that are regulated in cardiomyocytes in response to ET-1 for which Atf3 plays either a negative feedback or positive feed-forward role (Figure 3). Since loss of Atf3 results in a severely abnormal response to ET-1 (Figure 8), strict regulation of any or all of these targets must be important in ensuring an appropriate hypertrophic growth response. However, of all the potential targets, Egr1 emerged as a significant candidate and we provide substantial evidence that Atf3 is a transcriptional repressor for Egr1 in the ET-1 response. Thus Atf3 knockdown leads to sustained expression of *Egr1* mRNA and enhanced expression of Egr1 protein, and Atf3 binds directly to the Egr1 promoter. Furthermore, mathematical modelling of the system established that Atf3 alone can suffice to suppress *Egr1* mRNA expression.

Egr1 was among the first IEGs to be identified [42] and it is up-regulated in many cells in response to a wide range of growth stimuli [43]. As such, it is implicated in a host of different systems including kidney differentiation [44], macrophage differentiation [45], the nervous system and learning/memory [46,47], the immune response [48], wound healing and tissue repair [49], prostate cancer [50] and acute lung injury [51]. In the vascular system, Egr1 is associated with excessive smooth muscle cell proliferation resulting in in-stent restenosis following angioplasty [52]. Egr1 is also implicated in cardiac/cardiomyocyte hypertrophy. Thus expression of Egr1 is increased in cardiomyocytes and the heart in response to a variety of hypertrophic stimuli [27,28], and loss of Egr1 attenuates the hypertrophic response [29]. The importance of Egr1 in such a range of systems, together with the emergence of Atf3 as a negative feedback regulator and the co-regulation of the two genes in many situations, raises the possibility that the Atf3–Egr1 negative feedback loop is of broad general significance

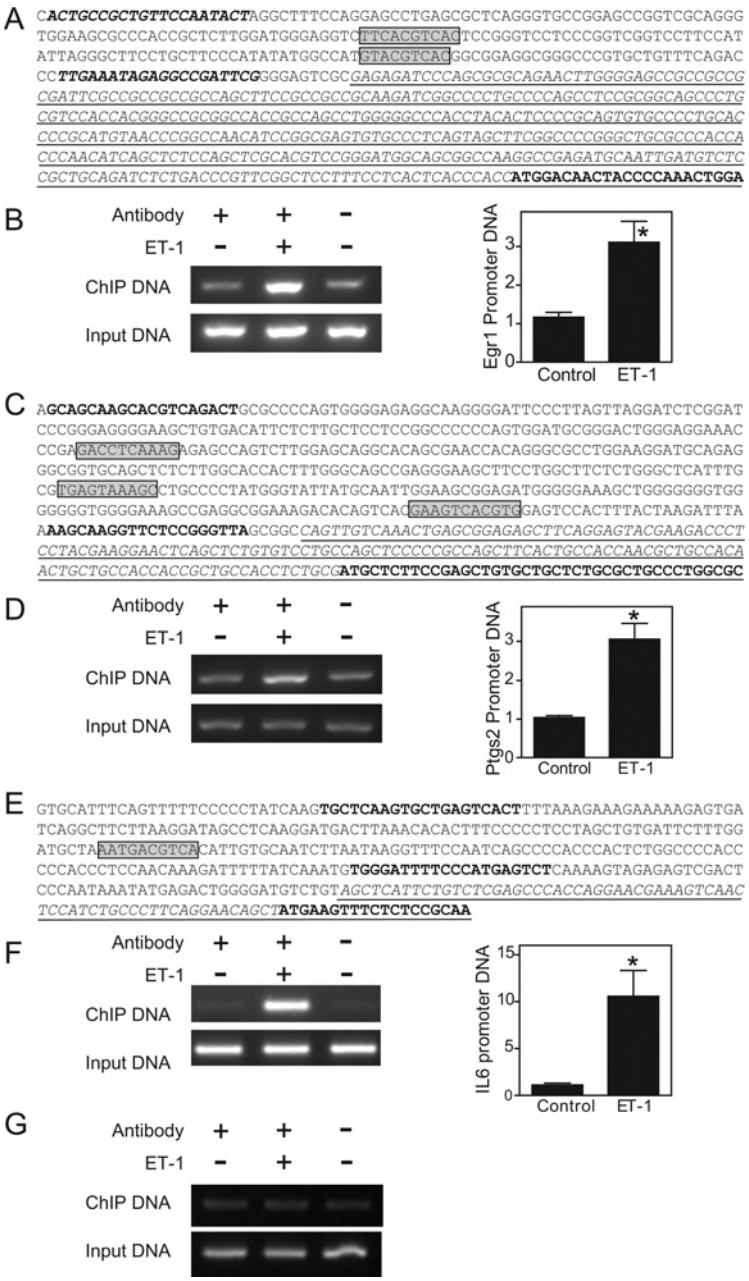

Figure 6 ChIP assays for binding of Atf3 to Egr1, Ptgs2 and IL6 promoters

Cardiomyocytes were unstimulated (control) or exposed to ET-1 (100 nM for 1 h). Promoter sequences with positions of PCR primers and potential Atf3-binding sites for Egr1 (**A**), Ptgs2 (**C**) and IL6 (**E**) are shown (coding sequence are in bold underlined text; 5′ untranslated regions are in underlined italics; positions of primers for PCR are in italic bold; and potential ATF/CRE-binding sites are shaded and boxed). ChIP was performed using antibodies against Atf3 with sqPCR across the Egr1 (**B**), Ptgs2 (**D**) and IL6 (**F**) promoters. Representative images for input DNA and ChIP DNA are provided (left-hand panels) with densitometric analysis (right-hand panels). Results are means ± S.E.M. for three myocyte preparations. $^*P < 0.05$ relative to control (Student's t test). (**G**) ChIP–PCR was performed for an unrelated sequence approximately 2000 bp downstream of the *IL6* gene. The experiment was repeated with similar results.

required to restrict expression of Egr1 and maintain a normal growth response.

Although Atf3 and Egr1 are co-regulated by a range of stimuli, their up-regulation is usually rapid and transient. As transcription factors, IEGs such as *Atf3* and *Egr1* are important in regulating downstream gene expression, and dysregulation leads to functional abnormalities and abnormal phenotypic responses. As demonstrated in the present study (Figure 8), cardiomyocyte hypertrophy cannot proceed normally in the absence of Atf3. This is not inconsistent with induction of cardiac hypertrophy in mice *in vivo* by overexpression of Atf3 [24]. Atf3 knockout also enhances cardiac hypertrophy induced by pressure overload in mice, but, in this model, MAPK signalling (including ERK1/2) induced by pressure overload is significantly enhanced [19] and this alone could account for enhanced hypertrophy [2,53]. Intriguing questions relate to how Atf3 modulates MAPK signalling and if the up-regulation of MAPK signalling is a compensatory mechanism for loss of Atf3. Other studies indicate that Atf3 is important in regulating, for example, the immune response [15,17], liver function [54] and pancreatic

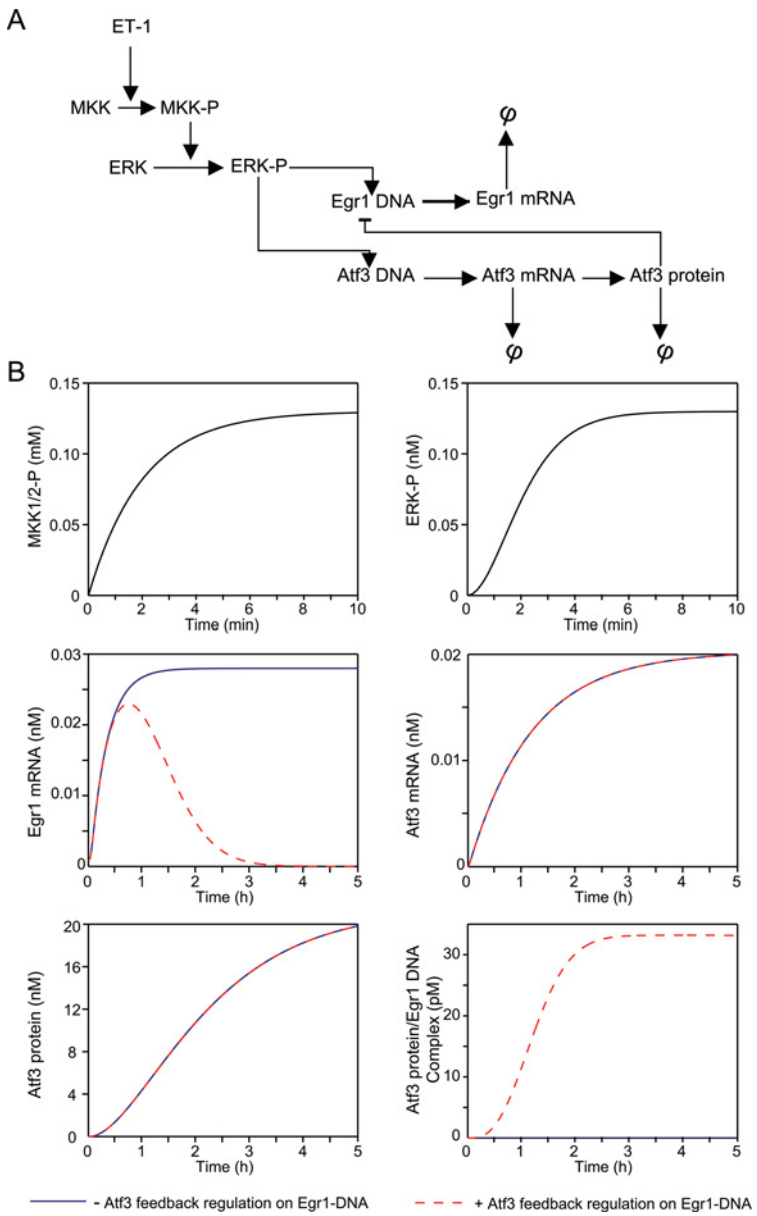

Figure 7 Mathematical modelling of the Atf3–Egr1 feedback system in the cardiomyocyte response to ET-1

(**A**) Schematic diagram of the system. ET-1 stimulates phosphorylation of MKK1/2 (MKK-P) which phosphorylates and activates ERK1/2 (ERK→ERK-P). Phosphorylated ERK binds to transcription factors (not shown) on the promoters of Egr1 and Atf3 (Egr1 DNA and Atf3 DNA) to promote transcription and production of *Egr1* mRNA and *Atf3* mRNA. *Atf3* mRNA is translated into Atf3 protein that eliminates the positive signal from phosphorylated ERK on the Egr1 promoter. φ denotes degradation. (**B**) Results from the mathematical model derived from (**A**) (see the Supplementary Online Data at http://www.BiochemJ.org/bj/444/bj4440343add.htm) to show the rates of accumulation of phosphorylated MKK1/2 (upper left-hand panel), phosphorylated ERK (upper right-hand panel), *Egr1* mRNA (centre left-hand panel), *Atf3* mRNA (centre right-hand panel), Atf3 protein (lower left-hand panel) and the Atf3 protein–Egr1 DNA complex (lower right-hand panel). The modelling was performed with (red broken line) or without (blue solid line) feedback regulation of Atf3 on the Egr1 promoter. No attempt was made to switch off either the initial signal from ERK1/2 or production of *Atf3* mRNA.

β-cell function [55,56]. Because of this, it is important to identify the genes that Atf3 regulates.

At least two previous studies took a systems approach to identify Atf3-regulated genes, neither of which identified Egr1 as a target. The first focused on TLR4 signalling and the effects of lipopolysaccharide on the macrophage transcriptome [15]. The strategy used Cytoscape (software that draws on published literature to identify protein–protein interactions) to predict Atf3-regulated genes from microarray data for subsequent experimental verification. Atf3 was particularly implicated in negative regulation of IL6. IL6 is up-regulated in cardiomyocytes by ET-1 as we have reported previously [57] and in the present study (Figure 4G). We have also previously reported preliminary data on the effects of AS-Atf3 AdV infection on *IL6* mRNA expression. In those experiments, low viral titres and a low MOI (<15) were used to suppress the increase in expression of Atf3 by 10 nM ET-1 (rather than 100 nM ET-1 used in the present study). As in the present study, AS-Atf3 AdVs enhanced the increase in *IL6* mRNA induced by ET-1 [57]. Our interpretation was that Atf3 suppressed IL6 transcription, consistent with the report on the role of Atf3 in the TLR4 response [15]. However, we know now that AdV infection has substantial effects on

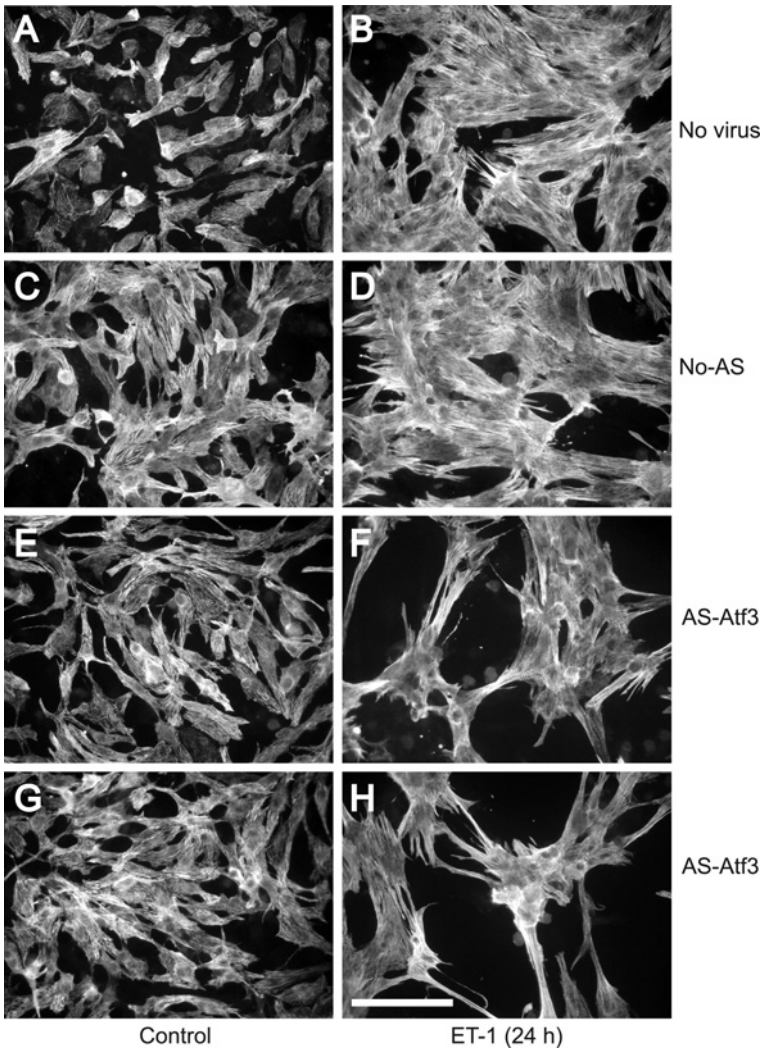

Figure 8 Atf3 is required for cardiomyocyte hypertrophy induced by ET-1

Cardiomyocytes were uninfected (**A** and **B**) or were infected with No-AS (**C** and **D**) or AS-Atf3 (**E**–**H**) AdVs, then unstimulated (Control; **A**, **C**, **E** and **G**) or exposed to 100 nM ET-1 for 24 h (**B**, **D**, **F** and **H**). Cells were immunostained with antibodies to troponin T. Results are representative of three independent experiments. Scale bar = 50 μm.

elements of the cardiomyocyte transcriptome and on IL6 in particular (Figure 2), and the data in the earlier report require re-interpretation. With submaximal virus and agonist concentrations (rather than the saturation levels used in the present study), slight differences between No-AS and AS-Atf3 viral titres were likely to be exaggerated. The No-AS AdV titre may have been slightly less than that of the AS-Atf3 AdVs and this could account for the significant effect of AS-Atf3 on *IL6* mRNA expression in control cells over and above that induced by the empty virus. We assumed that this indicated a basal effect of Atf3 on *IL6* mRNA expression. However, if the effect of AS-Atf3 in control cells is taken into account, ET-1 stimulation of *IL6* mRNA was similar (~4-fold) in cardiomyocytes infected with either No-AS or AS-Atf3 AdVs. We now therefore consider that Atf3 knockdown did not influence the increase in expression of *IL6* mRNA induced by ET-1. The lack of an effect of Atf3 knockdown on the increase in *IL6* mRNA expression induced by ET-1 in contrast with the TLR4 response probably reflects a fundamental difference in the signalling mechanisms. TLR4 signals predominantly through NF-κB and suppression of *IL6* expression by Atf3 results from its interaction with and inhibition of NF-κB [15]. ET-1 signals predominantly through ERK1/2 to up-regulate expression of IL6 [5]. With little/no signal through NF-κB, Atf3 is unlikely to inhibit transcription of *IL6*. However, Atf3 still binds to the *IL6* promoter (Figure 6G). It is less clear why *Egr1* was not identified as an Atf3-regulated gene in the TLR4 study [15]. One reason may be that Cytoscape is informed only by published data. Hence, the study focused on the Atf3–NFκB interaction and all validations centred on the NF-κB response.

The second study identifying Atf3-regulated genes focused on DNA damage in cancer cells. In that study, 5984 potential Atf3-binding promoters were identified in HCT116 colon cancer cells subjected to DNA damage and 1493 were identified in LNCaP prostate cancer cells exhibiting enhanced Atf3 expression [19]. In contrast with TLR4 signalling in macrophages [15], Atf3 plays a greater role in positive regulation of mRNA expression in these cancer cells, and there was no obvious effect of Atf3 knockdown on Egr1 expression. However, this paradigm differs radically from a growth response associated with IEG expression: Atf3 up-regulation is delayed (mRNA and protein expression are maximal at 6 and 12 h respectively) and potentially driven by p53 [58] with many of the Atf3-regulated genes being classic p53

targets [19]. It should also be considered that cancer cell lines were used rather than primary cells, and this may influence the signalling/gene expression response.

Since Atf3 and Egr1 are co-regulated in many systems, it is worth considering the extent to which the Atf3–Egr1 feedback mechanism operates. We expect it will apply in cardiomyocytes exposed to other stimuli that regulate gene expression primarily through MAPK signalling. We suggest that the Atf3–Egr1 negative feedback loop operates in other systems that also drive gene expression primarily through ERK1/2 signalling, but this awaits further investigation.

AUTHOR CONTRIBUTION

The present study was conceived and directed by Angela Clerk. Alejandro Giraldo and Oliver Barrett conducted the majority of the experimental work with equal contribution. Stephen Fuller constructed the vectors, produced the AdVs for the present study and, with Emre Amirak, assisted with parameterization of the model. Emre Amirak contributed microarray data and performed the qPCR experiments. The mathematical modelling was performed by Marcus Tindall with assistance from Bonhi Bhattacharya. Overall supervision of the present study was undertaken by Angela Clerk and Peter Sugden.

ACKNOWLEDGEMENTS

We thank Ross Bullivant and Joel Pearson for assistance in the initial phase of the mathematical modelling.

FUNDING

The work was funded by the British Heart Foundation [grant number PG/07/074/23445] and Fondation Leducq (Translatlantic Network of Excellence) [grant number CV05-02].

REFERENCES

1 Sugden, P. H. and Clerk, A. (1998) Cellular mechanisms of cardiac hypertrophy. J. Mol. Med. **76**, 725–746
2 Heineke, J. and Molkentin, J. D. (2006) Regulation of cardiac hypertrophy by intracellular signalling pathways. Nat. Rev. Mol. Cell Biol. **7**, 589–600
3 Clerk, A., Kemp, T. J., Zoumpoulidou, G. and Sugden, P. H. (2007) Cardiac myocyte gene expression profiling during H_2O_2-induced apoptosis. Physiol. Genomics **29**, 118–127
4 Kennedy, R. A., Kemp, T. J., Sugden, P. H. and Clerk, A. (2006) Using U0126 to dissect the role of the extracellular signal-regulated kinase 1/2 (ERK1/2) cascade in the regulation of gene expression by endothelin-1 in cardiac myocytes. J. Mol. Cell. Cardiol. **41**, 236–247
5 Cullingford, T. E., Markou, T., Fuller, S. J., Giraldo, A., Pikkarainen, S., Zoumpoulidou, G., Alsafi, A., Ekere, C., Kemp, T. J., Dennis, J. L. et al. (2008) Temporal regulation of expression of immediate early and second phase transcripts by endothelin-1 in cardiomyocytes. Genome Biol. **9**, R32
6 Marshall, A. K., Barrett, O. P., Cullingford, T. E., Shanmugasundram, A., Sugden, P. H. and Clerk, A. (2010) ERK1/2 signaling dominates over RhoA signaling in regulating early changes in RNA expression induced by endothelin-1 in neonatal rat cardiomyocytes. PLoS ONE **5**, e10027
7 Clerk, A., Gillespie-Brown, J., Fuller, S. J. and Sugden, P. H. (1996) Stimulation of phosphatidylinositol hydrolysis, protein kinase C translocation, and mitogen-activated protein kinase activity by bradykinin in ventricular myocytes. Dissociation from the hypertrophic response. Biochem. J. **317**, 109–118
8 Hai, T. and Hartman, M. G. (2001) The molecular biology and nomenclature of the activating transcription factor/cAMP responsive element binding family of transcription factors: activating transcription factor proteins and homeostasis. Gene **273**, 1–11
9 Lu, D., Chen, J. and Hai, T. (2007) The regulation of *ATF3* gene expression by mitogen-activated protein kinases. Biochem. J. **401**, 559–567
10 Mayer, S. I., Dexheimer, V., Nishida, E., Kitajima, S. and Thiel, G. (2008) Expression of the transcriptional repressor ATF3 in gonadotrophs is regulated by Egr-1, CREB, and ATF2 after gonadotropin-releasing hormone receptor stimulation. Endocrinology **149**, 6311–6325
11 Tamura, K., Hua, B., Adachi, S., Guney, I., Kawauchi, J., Morioka, M., Tamamori-Adachi, M., Tanaka, Y., Nakabeppu, Y., Sunamori, M. et al. (2005) Stress response gene *ATF3* is a target of c-myc in serum-induced cell proliferation. EMBO J. **24**, 2590–2601
12 Yamaguchi, K., Lee, S. H., Kim, J. S., Wimalasena, J., Kitajima, S. and Baek, S. J. (2006) Activating transcription factor 3 and early growth response 1 are the novel targets of LY294002 in a phosphatidylinositol 3-kinase-independent pathway. Cancer Res. **66**, 2376–2384
13 Bottone, F. G., Moon, Y., Alston-Mills, B. and Eling, T. E. (2005) Transcriptional regulation of activating transcription factor 3 involves the early growth response-1 gene. J. Pharmacol. Exp. Ther. **315**, 668–677
14 Wolfgang, C. D., Liang, G., Okamoto, Y., Allen, A. E. and Hai, T. (2000) Transcriptional autorepression of the stress-inducible gene *ATF3*. J. Biol. Chem. **275**, 16865–16870
15 Gilchrist, M., Thorsson, V., Li, B., Rust, A. G., Korb, M., Roach, J. C., Kennedy, K., Hai, T., Bolouri, H. and Aderem, A. (2006) Systems biology approaches identify ATF3 as a negative regulator of Toll-like receptor 4. Nature **441**, 173–178
16 Whitmore, M. M., Iparraguirre, A., Kubelka, L., Weninger, W., Hai, T. and Williams, B. R. (2007) Negative regulation of TLR-signaling pathways by activating transcription factor-3. J. Immunol. **179**, 3622–3630
17 Thompson, M. R., Xu, D. and Williams, B. R. (2009) ATF3 transcription factor and its emerging roles in immunity and cancer. J. Mol. Med. **87**, 1053–1060
18 Wang, J., Cao, Y. and Steiner, D. F. (2003) Regulation of proglucagon transcription by activated transcription factor (ATF) 3 and a novel isoform, ATF3b, through the cAMP-response element/ATF site of the proglucagon gene promoter. J. Biol. Chem. **278**, 32899–32904
19 Tanaka, Y., Nakamura, A., Morioka, M. S., Inoue, S., Tamamori-Adachi, M., Yamada, K., Taketani, K., Kawauchi, J., Tanaka-Okamoto, M., Miyoshi, J. et al. (2011) Systems analysis of ATF3 in stress response and cancer reveals opposing effects on pro-apoptotic genes in p53 Pathway. PLoS ONE **6**, e26848
20 Nobori, K., Ito, H., Tamamori-Adachi, M., Adachi, S., Ono, Y., Kawauchi, J., Kitajima, S., Marumo, F. and Isobe, M. (2002) ATF3 inhibits doxorubicin-induced apoptosis in cardiac myocytes: a novel cardioprotective role of ATF3. J. Mol. Cell. Cardiol. **34**, 1387–1397
21 Markou, T., Marshall, A. K., Cullingford, T. E., Tham, E. L., Sugden, P. H. and Clerk, A. (2010) Regulation of the cardiomyocyte transcriptome vs translatome by endothelin-1 and insulin: translational regulation of 5′ terminal oligopyrimidine tract (TOP) mRNAs by insulin. BMC Genomics **11**, 343
22 Kim, M. Y., Seo, E. J., Lee, D. H., Kim, E. J., Kim, H. S., Cho, H. Y., Chung, E. Y., Lee, S. H., Baik, E. J., Moon, C. H. and Jung, Y. S. (2010) Gadd45β is a novel mediator of cardiomyocyte apoptosis induced by ischaemia/hypoxia. Cardiovasc. Res. **87**, 119–126
23 Liu, L., Zhu, J., Glass, P. S., Brink, P. R., Rampil, I. J. and Rebecchi, M. J. (2009) Age-associated changes in cardiac gene expression after preconditioning. Anesthesiology **111**, 1052–1064
24 Okamoto, Y., Chaves, A., Chen, J., Kelley, R., Jones, K., Weed, H. G., Gardner, K. L., Gangi, L., Yamaguchi, M., Klomkleaw, W. et al. (2001) Transgenic mice with cardiac-specific expression of activating transcription factor 3, a stress-inducible gene, have conduction abnormalities and contractile dysfunction. Am. J. Pathol. **159**, 639–650
25 Dorn, II, G. W., Robbins, J. and Sugden, P. H. (2003) Phenotyping hypertrophy: eschew obfuscation. Circ. Res. **92**, 1171–1175
26 Zhou, H., Shen, D. F., Bian, Z. Y., Zong, J., Deng, W., Zhang, Y., Guo, Y. Y., Li, H. and Tang, Q. Z. (2011) Activating transcription factor 3 deficiency promotes cardiac hypertrophy, dysfunction, and fibrosis induced by pressure overload. PLoS ONE **6**, e26744
27 Iwaki, K., Sukhatme, V. P., Shubeita, H. E. and Chien, K. R. (1990) α- and β-Adrenergic stimulation induces distinct patterns of immediate early gene expression in neonatal rat myocardial cells. *fos/jun* expression is associated with sarcomere assembly; *Egr*-1 induction is primarily an α_1-mediated response. J. Biol. Chem. **265**, 13809–13817
28 Neyses, L. and Pelzer, T. (1995) The biological cascade leading to cardiac hypertrophy. Eur. Heart J. **16**, 8–11
29 Saadane, N., Alpert, L. and Chalifour, L. E. (2000) Altered molecular response to adrenoreceptor-induced cardiac hypertrophy in Egr-1-deficient mice. Am. J. Physiol. Heart Circ. Physiol. **278**, H796–H805
30 Clerk, A. and Sugden, P. H. (1997) Cell stress-induced phosphorylation of ATF2 and c-Jun transcription factors in rat ventricular myocytes. Biochem. J. **325**, 801–810
31 Sugden, P. H., Markou, T., Fuller, S. J., Tham, E. L., Molkentin, J. D., Paterson, H. F. and Clerk, A. (2011) Monophosphothreonyl extracellular signal-regulated kinases 1 and 2 (ERK1/2) are formed endogenously in intact cardiac myocytes and are enzymically active. Cell. Signalling **23**, 468–477
32 Meyer, R. G., Kupper, J. H., Kandolf, R. and Rodemann, H. P. (2002) Early growth response-1 gene (*Egr-1*) promoter induction by ionizing radiation in U87 malignant glioma cells *in vitro*. Eur. J. Biochem. **269**, 337–346
33 Xie, W., Fletcher, B. S., Andersen, R. D. and Herschman, H. R. (1994) v-Src induction of the TIS10/PGS2 prostaglandin synthase gene is mediated by an ATF/CRE transcription response element. Mol. Cell. Biol. **14**, 6531–6539
34 Xie, W. and Herschman, H. R. (1995) v-Src induces prostaglandin synthase 2 gene expression by activation of the c-Jun N-terminal kinase and the c-Jun transcription factor. J. Biol. Chem. **270**, 27622–27628

35 Ben-Ari, Y., Brody, Y., Kinor, N., Mor, A., Tsukamoto, T., Spector, D. L., Singer, R. H. and Shav-Tal, Y. (2010) The life of an mRNA in space and time. J. Cell Sci. **123**, 1761–1774

36 Maiuri, P., Knezevich, A., De Marco, A., Mazza, D., Kula, A., McNally, J. G. and Marcello, A. (2011) Fast transcription rates of RNA polymerase II in human cells. EMBO Rep. **12**, 1280–1285

37 Clerk, A., Michael, A. and Sugden, P. H. (1998) Stimulation of the p38 mitogen-activated protein kinase pathway in neonatal rat ventricular myocytes by the G protein-coupled receptor agonists, endothelin-1 and phenylephrine: a role in cardiac myocyte hypertrophy? J. Cell Biol. **142**, 523–535

38 Clerk, A., Aggeli, I.-K. S., Stathopoulou, K. and Sugden, P. H. (2006) Peptide growth factors signal differentially through protein kinase C to extracellular signal-regulated kinases in neonatal cardiomyocytes. Cell. Signalling **18**, 225–235

39 Nagashima, T., Shimodaira, H., Ide, K., Nakakuki, T., Tani, Y., Takahashi, K., Yumoto, N. and Hatakeyama, M. (2007) Quantitative transcriptional control of ErbB receptor signaling undergoes graded to biphasic response for cell differentiation. J. Biol. Chem. **282**, 4045–4056

40 Uzonyi, B., Lotzer, K., Jahn, S., Kramer, C., Hildner, M., Bretschneider, E., Radke, D., Beer, M., Vollandt, R., Evans, J. F. et al. (2006) Cysteinyl leukotriene 2 receptor and protease-activated receptor 1 activate strongly correlated early genes in human endothelial cells. Proc. Natl. Acad. Sci. U.S.A **103**, 6326–6331

41 Schweighofer, B., Testori, J., Sturtzel, C., Sattler, S., Mayer, H., Wagner, O., Bilban, M. and Hofer, E. (2009) The VEGF-induced transcriptional response comprises gene clusters at the crossroad of angiogenesis and inflammation. Thromb. Haemost. **102**, 544–554

42 Sukhatme, V. P., Cao, X., Chang, L. C., Tsai-Morris, C., Stamenkovich, D., Ferreira, P. C. P., Cohen, D. R., Edwards, S. A., Shows, T. B., Curran, T. et al. (1988) A zinc finger-encoding gene coregulated with c-*fos* during growth and differentiation, and after cellular depolarization. Cell **53**, 37–43

43 Sukhatme, V. P. (1990) Early transcriptional events in cell growth: the Egr family. J. Am. Soc. Nephrol. **1**, 859–866

44 Sukhatme, V. P. (1992) The Egr transcription factor family: from signal transduction to kidney differentiation. Kidney Int. **41**, 550–553

45 Liebermann, D. A. and Hoffman, B. (1994) Differentiation primary response genes and proto-oncogenes as positive and negative regulators of terminal hematopoietic cell differentiation. Stem Cells **12**, 352–369

46 Beckmann, A. M. and Wilce, P. A. (1997) Egr transcription factors in the nervous system. Neurochem. Int. **31**, 477–510

47 Walton, M., Henderson, C., Mason-Parker, S., Lawlor, P., Abraham, W. C., Bilkey, D. and Dragunow, M. (1999) Immediate early gene transcription and synaptic modulation. J. Neurosci. Res. **58**, 96–106

48 McMahon, S. B. and Monroe, J. G. (1996) The role of early growth response gene 1 (*egr-1*) in regulation of the immune response. J. Leukoc. Biol. **60**, 159–166

49 Braddock, M. (2001) The transcription factor Egr-1: a potential drug in wound healing and tissue repair. Ann. Med. **33**, 313–318

50 Adamson, E. D. and Mercola, D. (2002) Egr1 transcription factor: multiple roles in prostate tumor cell growth and survival. Tumour Biol. **23**, 93–102

51 Ngiam, N., Post, M. and Kavanagh, B. P. (2007) Early growth response factor-1 in acute lung injury. Am. J. Physiol Lung Cell. Mol. Physiol. **293**, L1089–L1091

52 Khachigian, L. M. (2001) Catalytic oligonucleotides targeting EGR-1 as potential inhibitors of in-stent restenosis. Ann. N. Y. Acad. Sci. **947**, 412–415

53 Clerk, A., Cullingford, T. E., Fuller, S. J., Giraldo, A., Markou, T., Pikkarainen, S. and Sugden, P. H. (2007) Signaling pathways mediating cardiac myocyte gene expression in physiological and stress responses. J. Cell. Physiol. **212**, 311–322

54 Allen-Jennings, A. E., Hartman, M. G., Kociba, G. J. and Hai, T. (2002) The roles of ATF3 in liver dysfunction and the regulation of phosphoenolpyruvate carboxykinase gene expression. J. Biol. Chem. **277**, 20020–20025

55 Zmuda, E. J., Qi, L., Zhu, M. X., Mirmira, R. G., Montminy, M. R. and Hai, T. (2010) The roles of ATF3, an adaptive-response gene, in high-fat-diet-induced diabetes and pancreatic α-cell dysfunction. Mol. Endocrinol. **24**, 1423–1433

56 Zmuda, E. J., Viapiano, M., Grey, S. T., Hadley, G., Garcia-Ocana, A. and Hai, T. (2010) Deficiency of *Atf3*, an adaptive-response gene, protects islets and ameliorates inflammation in a syngeneic mouse transplantation model. Diabetologia **53**, 1438–1450

57 Clerk, A., Cullingford, T. E., Fuller, S. J., Giraldo, A. and Sugden, P. H. (2009) Endothelin-1 regulation of immediate early gene expression in cardiac myocytes: negative feedback regulation of interleukin 6 by Atf3 and Klf2. Adv. Enzyme Regul. **49**, 30–42

58 Fan, F., Jin, S., Amundson, S. A., Tong, T., Fan, W., Zhao, H., Zhu, X., Mazzacurati, L., Li, X., Petrik, K. L. et al. (2002) ATF3 induction following DNA damage is regulated by distinct signaling pathways and over-expression of ATF3 protein suppresses cells growth. Oncogene **21**, 7488–7496

Received 19 January 2012/29 February 2012; accepted 5 March 2012
Published as BJ Immediate Publication 5 March 2012, doi:10.1042/BJ20120125

Biochem. J. (2012) **444**, 343–355 (Printed in Great Britain) doi:10.1042/BJ20120125

online data

SUPPLEMENTARY ONLINE DATA

Feedback regulation by Atf3 in the endothelin-1-responsive transcriptome of cardiomyocytes: Egr1 is a principal Atf3 target

Alejandro GIRALDO*[1], Oliver P. T. BARRETT†[1], Marcus J. TINDALL*‡, Stephen J. FULLER*, Emre AMIRAK*, Bonhi S. BHATTACHARYA‡, Peter H. SUGDEN* and Angela CLERK*[2]

*Institute of Cardiovascular and Metabolic Research, School of Biological Sciences, University of Reading, Whiteknights, PO Box 218, Reading RG6 6BX, U.K., †Department of Life Sciences, Imperial College London, London SW7 2AZ, U.K., and ‡Department of Mathematics and Statistics, University of Reading, Whiteknights, PO Box 220, Reading RG6 6AX, U.K.

METHODS

Reaction equations

The reaction equations governing the expression of *Egr1* and *Atf3* mRNA, Atf3 protein and subsequent suppression of *Egr1* mRNA expression by Atf3 protein are described as follows. Each of the following processes occur at the rate indicated. Further details on these can be found in Table S1. -P denotes a phosphorylated version of the protein.

The phosphorylation of MKK by ET-1 is denoted by:

$$\text{ET-1} + \text{MKK} \xrightarrow{k_1} \text{ET-1} + \text{MKK-P} \tag{1}$$

which subsequently phosphorylates the unphosphorylated ERK:

$$\text{MKK-P} + \text{ERK} \xrightarrow{k_2} \text{MKK-P} + \text{ERK-P} \tag{2}$$

ERK-P is now free to transcribe both *Egr1* and *Atf3* mRNA such that:

$$\text{ERK-P} + \text{DNA}_{\text{Egr1}} \underset{k_{-3}}{\overset{k_3}{\rightleftharpoons}} \text{ERK-P} \cdot \text{DNA}_{\text{Egr1}} \xrightarrow{k_4} \text{mRNA}_{\text{Egr1}} \tag{3}$$

and:

$$\text{ERK-P} + \text{DNA}_{\text{Atf3}} \underset{k_{-5}}{\overset{k_5}{\rightleftharpoons}} \text{ERK-P} \cdot \text{DNA}_{\text{Atf3}} \xrightarrow{k_6} \text{mRNA}_{\text{Atf3}} \tag{4}$$

which are both degraded:

$$\text{mRNA}_{\text{Egr1}} \xrightarrow{d_1} \phi, \qquad \text{mRNA}_{\text{Atf3}} \xrightarrow{d_2} \phi \tag{5}$$

Here $\cdot$ denotes a complex and ϕ the degraded mRNA.

The suppression of *Egr1* mRNA transcription by Atf3 is described by:

$$\text{ERK-P} \cdot \text{DNA}_{\text{Egr1}} + \text{Atf3} \xrightarrow{k_7} \text{Atf3} \cdot \text{DNA}_{\text{Egr1}} \tag{6}$$

where the concentration of ERK-P is considered to be in excess.

Finally the translation of *Atf3* mRNA to Atf3 protein and subsequent degradation of the protein are denoted by:

$$\text{mRNA}_{\text{Atf3}} \xrightarrow{k_8} \text{Atf3} \quad \text{and} \quad \text{Atf3} \xrightarrow{d_3} \phi_P \tag{7}$$

respectively, where ϕ_P denotes degraded protein. In the present study we do not explicitly account for the degraded mRNAs or Atf3 protein.

Mathematical model

The Law of Mass Action [6] was applied to eqns (1)–(7). This led to the following system of nonlinear ordinary differential equations:

$$\frac{dm}{dt} = -k_1 e_t m \tag{8}$$

$$\frac{dm_P}{dt} = k_1 e_t m \tag{9}$$

$$\frac{dE}{dt} = -k_2 m_P E \tag{10}$$

$$\frac{dE_P}{dt} = k_2 m_P E - k_3 E_P D_E + k_{-3} T_E - k_5 E_P D_A + k_{-5} T_A \tag{11}$$

$$\frac{dD_E}{dt} = -k_3 E_P D_E + k_{-3} T_E \tag{12}$$

$$\frac{dT_E}{dt} = k_3 E_P D_E - k_{-3} T_E - k_7 T_E A \tag{13}$$

$$\frac{dM_E}{dt} = k_4 T_E - d_1 M_E \tag{14}$$

$$\frac{dD_A}{dt} = -k_5 E_P D_A + k_{-5} T_A \tag{15}$$

$$\frac{dT_A}{dt} = k_5 E_P D_A - k_{-5} T_A \tag{16}$$

$$\frac{dM_A}{dt} = k_6 T_A - d_2 M_A \tag{17}$$

$$\frac{dA}{dt} = k_8 M_A - k_7 T_E A - d_3 A \tag{18}$$

$$\frac{dS}{dt} = k_7 T_E A \tag{19}$$

Each of the variables is defined as follows: e_T represents the concentration of ET-1 (denoted $e_T = [\text{ET-1}]$), $m = [\text{MKK}]$, $m_P = [\text{MKK-P}]$, $E = [\text{ERK}]$, $E_P = [\text{ERK-P}]$, $D_E = [\text{DNA}_{\text{Egr1}}]$, $D_A = [\text{DNA}_{\text{Atf3}}]$, $T_E = \text{ERK-P}{\cdot}\text{DNA}_{\text{Egr1}}$, $T_A = \text{ERK-P}{\cdot}\text{DNA}_{\text{Atf3}}$, $M_E = [\text{mRNA}_{\text{Egr1}}]$, $M_A = [\text{mRNA}_{\text{Atf3}}]$, $S = [\text{Atf3}{\cdot}\text{DNA}_{\text{Egr1}}]$ and

[1] These authors contributed equally to this work.
[2] To whom correspondence should be addressed (email a.clerk@reading.ac.uk).

$A = [\text{Atf3}]$. In the present study the concentration of ET-1 is assumed to be constant. The rate of Atf3 protein to Egr1 DNA binding is assumed to be immediate and no delays are incurred in this process.

The system is closed with the initial conditions:

$$m = m_0,\ m_P = 0,\ E = E_0,\ E_P = 0,\ D_E = D_{E0},\ T_E = 0,$$
$$M_E = M_{E0},\ D_A = D_{A0},\ T_A = 0,\ M_A = 0,\ A = 0 \text{ and}$$
$$S = 0 \tag{20}$$

which state that MKK and ERK are initially assumed to be unphosphorylated, the concentration of *Egr1* mRNA is non-zero whereas no *Atf3* mRNA, Atf3 protein or any of the complexes have been created.

The governing system of equations can be simplified as follows. Addition of eqns (8) and (9), integration with respect to time and application of the respective initial conditions yields the conservation relation:

$$m + m_P = m_0 \tag{21}$$

Substituting for m into eqn (9), integrating and applying the initial condition yields:

$$m_P(t) = m_0\left(1 - e^{-k_1 e_T t}\right) \tag{22}$$

Addition of eqns (12), (13) and (19), integration with respect to t and application of the initial conditions yields.

$$D_E + T_E + S = D_{E0} \tag{23}$$

Likewise for eqns (15) and (16):

$$D_A + T_A = D_{A0} \tag{24}$$

Assuming eqn (16) is quasi-steady and substituting for D_A using eqn (24) leads to:

$$T_A \simeq \frac{D_{A0} E_P}{E_P + K_5} \tag{25}$$

where $K_5 = k_{-5}/k_5$.

Bringing all these results together gives:

$$m_P(t) = m_0\left(1 - e^{-k_1 e_T t}\right) \tag{26}$$

$$\frac{dE}{dt} = -k_2 m_P E \tag{27}$$

$$\frac{dE_P}{dt} = k_2 m_P E - k_3 E_P(D_{E0} - T_E - S) + k_{-3} T_E \tag{28}$$

$$\frac{dT_E}{dt} = k_3 E_P(D_{E0} - T_E - S) - k_{-3} T_E - k_7 T_E A \tag{29}$$

$$\frac{dM_E}{dt} = k_4 T_E - d_1 M_E \tag{30}$$

$$\frac{dM_A}{dt} = \frac{k_6^* E_P}{E_P + K_5} - d_2 M_A \tag{31}$$

$$\frac{dA}{dt} = k_8 M_A - k_7 T_E A - d_3 A \tag{32}$$

$$\frac{dS}{dt} = k_7 T_E A \tag{33}$$

with the initial conditions:

$$E = E_0, \quad E_P = 0, \quad T_E = 0, \quad M_E = M_{E0}, \quad M_A = 0,$$
$$A = 0 \quad \text{and} \quad S = 0 \tag{34}$$

where $k_6^* = k_6 D_{A0}$. When Egr1 transcription is not suppressed by Atf3 protein we have $k_7 = 0$.

Parameterization

The mathematical model has been informed with data available within the literature, from our own previous studies as well the present study. A complete list of the parameter values used can be found in Table S1. In cases where parameter values have been derived these are explained as follows.

Estimation of the activation rate of MKK and ERK

The time course for activation of ERK1 was determined previously [9] and maximal activation was at 3 min. The time course for activation of MKK was determined by immunoblotting with antibodies against phosphorylated (i.e. activated) MKK (Cell Signaling Technology). A representative blot is shown in Figure S1. The time course for activation by a range of agonists (epidermal growth factor, ET-1, phorbol 12-myristate 13-acetate or platelet-derived growth factor) all showed maximal activation by 2–3 min. We therefore assumed the time to maximal activation of MKK to be 2 min with a further 1 min for maximal activation of ERK.

The concentration of MKK in cardiomyocytes was estimated by immunoblotting cardiomyocyte extracts from a known number of cells alongside known concentrations of recombinant MKK1. Antibodies against total MKK were from Cell Signaling Technology. Following densitometric analysis, a standard curve was constructed from which the amount of MKK in the myocyte extract was estimated. The concentration was calculated on the basis of the estimated volume of a neonatal myocyte. The concentration of ERK was assumed to be similar to MKK given that this lies within the range seen in other cells [4].

$k_1 e_t$: Rate of MKK activation by ET-1

The time taken for maximal activation of MKK by ET-1 is 2 min, thus:

$$k_1 e_t = \frac{1}{120\ \text{s}} = 8.30 \times 10^{-3}\ \text{s}^{-1}$$

k_2: Rate of ERK activation by MKK

The time taken to activate ERK by MKK is 60 s, so:

$$k_2 E = \frac{1}{60\ \text{s}} = 1.67 \times 10^{-2}\ \text{s}^{-1}$$

The total ERK concentration is 130 nM such that:

$$k_2 = 1.28 \times 10^5\ (\text{Ms})^{-1}$$

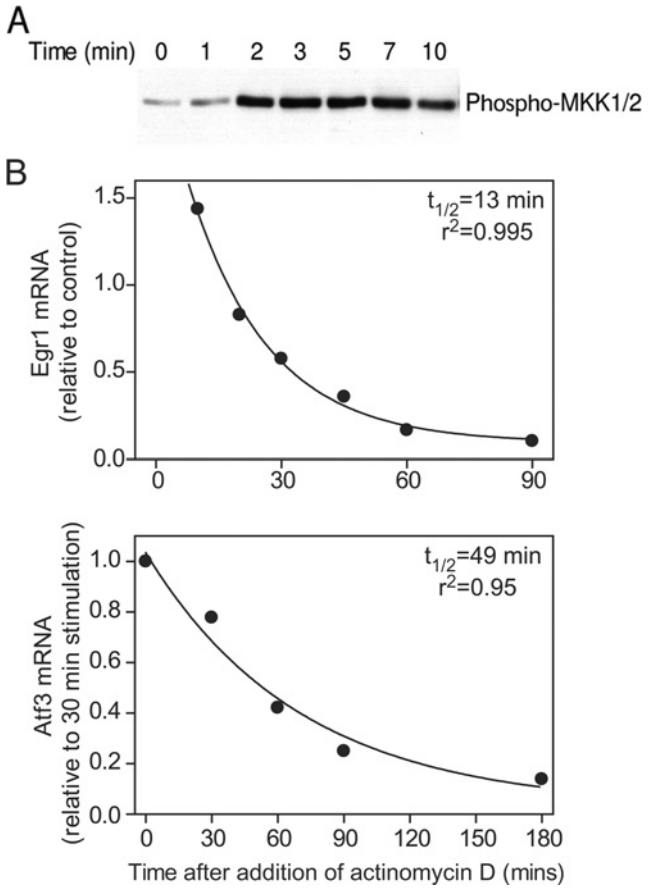

Figure S1 Activation of MKK phosphorylation by ET-1 (A) and effect of actinomycin D on Egr1 and Atf3 transcription (B)

(**A**) Cardiomyocytes were exposed to ET-1 for the times indicated. Protein extracts were immunoblotted with antibodies to phospho-MKK. A representative image is shown. (**B**) Cardiomyocytes were stimulated for 30 min before addition of actinomycin D (4μM) to inhibit transcription. Expression of Egr1 (upper panel) or Atf3 (lower panel) mRNAs were measured by qPCR at the indicated times after actinomycin D addition. A one-phase exponential curve was fitted using GraphPad Prism 4.

k_4^*, k_6^*: Egr1 and Atf3 transcription rates

The size of the Atf3 and Egr1 genes, mRNAs and proteins were for mouse (for rat, the 5′ untranslated region was not defined for Egr1 and the rat genome is not well sequenced in the intronic regions for Atf3). Sequences were obtained from the NCBI. For *Atf3* (Gene ID: 11910), this gives a total gene length of 13 038 base pairs (bp), a 5′ untranslated region of 62 nucleotides and protein of 181 amino acids. For *Egr1* (Gene ID: 13653), this gives a total gene length of 3750 bp. To estimate the rate of transcription, the total length of the gene was used allowing for an additional 200 nucleotides to be transcribed before termination. The maximum rate of transcription has been estimated recently to range from 55 bases/s to greater than 800 bases/s [1,5]. Thus to transcribe one molecule of mRNA from one gene, assuming a rate of 55 bases/s, takes:

$$\frac{3950 \text{ bases}}{55 \text{ bases/s}} = 71.82 \text{ s}$$

Per gene, this equates to 1.39×10^{-2} molecules mRNA s^{-1}. Since a cell contains two genes, we have 2.78×10^{-2} molecules of *Egr1* mRNA being synthesized per cell per s. Taking the cell volume of 6.7 pl we obtain:

$$k_4^* = \frac{2.78 \times 10^{-2} \text{ molecules} \cdot \text{s}^{-1}}{6.7 \times 10^{-9} \text{ ml}}$$
$$= 4.15 \times 10^5 \text{ molecules} \cdot \text{ml}^{-1} \cdot \text{s}^{-1} = 6.89 \times 10^{-16} \text{ Ms}^{-1} \quad (35)$$

We can undertake a similar calculation for Atf3 transcription to obtain:

$$k_6^* = 5.15 \times 10^{-15} \text{ Ms}^{-1}$$

k_8: Atf3 translation rate

The rate of translation of Atf3 was estimated on the basis of scanning of the 5′ untranslated region at a rate of six nucleotides/s [11], translation of the coding sequence at a rate of 20 amino acids/s (N.B. the reported rate of translation is in the range of 4–20 amino acids/s [10,12] and we presume translation of IEGs is efficient) with five ribosomes attached simultaneously to each mRNA (N.B. the predicted occupancy is one ribosome per 32 amino acids) [7].

K_5 and k_3, k_{-3}: ERK-P dissociation rates for Egr1 and Atf3 DNA

The model is based on the assumption that phospho-ERK bind to transcription factors that are pre-bound to the Atf3 and Egr1 promoters and this drives transcription. We presume that the ERK binding is mediated through a DEF motif with an estimated dissociation rate of 0.5 μM (the dissociation rate for Elk1 is 0.25 μM; that for Fos is 1 μM) [2]. Given that $K_3 = k_{-3}/k_3$, we use an initial estimate of $k_{-3} = 5 \times 10^{-2}$/s to obtain $k_3 = 1 \times 10^5$ $(\text{Ms})^{-1}$.

d_1, d_2, d_3: Degradation rates of Egr1 mRNA, Atf3 mRNA and Atf3 protein

To estimate the half-life of *Egr1* and *Atf3* mRNA, cardiomyocytes were exposed to ET-1 for 30 min then incubated without or with actinomycin D (4 μM, added directly to the culture dish). Cells were harvested at the indicated times following addition of actinomycin D and mRNA expression was measured by qPCR. GraphPad Prism 4 was used to fit a one-phase exponential decay curve to the data shown in Figure S1, giving a half-life of 13 min for Egr1 and 49 min for Atf3. The rate of degradation is defined by:

$$d = \frac{\ln 2}{t_{1/2}}$$

which leads to:

$$d_1 = 8.89 \times 10^{-4} \text{ s}^{-1} \text{ and } d_2 = \frac{\ln 2}{2580 \text{ s}} = 2.36 \times 10^{-4} \text{s}^{-1} \quad (36)$$

We assume Atf3 protein degrades at the same rate as *Atf3* mRNA.

Egr1 DNA concentration

We assume there are two molecules of DNA per cell. The volume of a neonatal myocyte was estimated given that an adult myocyte has a volume of 34 pl with a capacitance of 66 pF [3,8] and the capacitance of a neonatal myocyte is 13 pF [8]. This gives 6.7 pl per cell leading to concentration of 33.2 pM.

Table S1 Model parameter values

Parameter	Definition	Value
m_0	Total MKK	130 nM
E_0	Total ERK	130 nM
M_{E0}	Initial Egr1 mRNA concentration	1 pM
D_{e0}	Egr1 DNA concentration	33.2 pM
$k_1 e_t$	Rate of MKK activation by ET-1	8.30×10^{-3} s^{-1}
k_2	Rate of ERK activation by MKK	1.28×10^5(Ms)$^{-1}$
k_3	Rate of ERK-P activation of Egr1 DNA	1.00×10^5(Ms)$^{-1}$
k_{-3}	Rate of ERK-P reverse activation of Egr1 DNA	5.00×10^{-2}(Ms)$^{-1}$
k_4^*	*Egr1* mRNA transcription rate	6.89×10^{-15} M/s
k_6^*	*Atf3* mRNA transcription rate	1.03×10^{-15} M/s
k_7	Atf3 supression rate	To be determined
k_8	Atf3 translation rate	0.25 s^{-1}
K_5	ERK-P and Atf3 DNA dissociation rate	0.5×10^{-6} M
d_1	Degradation rate of *Atf3* mRNA	8.89×10^{-4} s^{-1}
d_2	Degradation rate of *Egr1* mRNA	2.36×10^{-4} s^{-1}
d_3	Degradation rate of Atf3 protein	2.36×10^{-4} s^{-1}

RESULTS

The governing system of nonlinear ordinary differential equations (ODEs) (eqns 27–33) was solved using Gear's method available in Matlab (The Mathworks, Version 7.11) via the solver ode15, with $m_P(t)$ given by eqn (26).

Using the parameter values detailed in Table S1 we found the 20-fold change in *Egr1* mRNA determined experimentally could not be reproduced using these values [using an initial estimate of $k_7 = 1 \times 10^5$ (Ms)$^{-1}$]. As such we undertook a sensitivity analysis in which we varied the rates of *Egr1* and *Atf3* mRNA transcription (k_4^*,k_6^*), ERK-P reverse activation of Egr1 DNA (k_{-3}) and the ERK-P association rate for Atf3 DNA (K_3). The most appropriate variation in these values which gave a good fit to the data was found to be a 5-fold increase in both the transcription rates of *Egr1* and *Atf3* mRNA ($5 \times k_4^*$,$5 \times k_6^*$), a 10-fold decrease in the rate of ERK-P dissociation for Egr1 DNA (k_{-3}/10) and a 50-fold decrease in the ERK-P association rate for Atf3 DNA (K_3/50). Such a variation in the rates of Egr1 and Atf3 transcription is equivalent to a rate of 275 bases/s rather than the original assumption of 55 bases/s. Such a variation lies within the range recently reported in [1] and [5].

This led to a very good fit to the experimental data in terms of the magnitude variation in *Egr1* mRNA observed experimentally and a relatively good fit (qualitatively) to the supression of *Egr1* mRNA by Atf3. To further improve this model-data fit we adjusted the rate of Atf3 suppression (k_7). Good fits to the data were obtained for the range of values 1.00×10^5 (Ms)$^{-1} \leqslant k_7 \leqslant 6 \times 10^5$ (Ms)$^{-1}$.

Table S2 Primers used for qPCR and sqPCR

mRNA sequences were from the Rat Genome Database (http://www.ncbi.nlm.nih.gov/entrez).

Gene symbol (GenBank® accession number)	Size (bp)	Forward primer (position in sequence)	Reverse primer (position in sequence)
(a) qPCR primers			
Atf3 (NM_012912.1)	108	5′-TCGCCATCCAGAACAAGCA-3′ (140–158)	5′-GGGCCACCTCAGACTTGGT-3′ (229–247)
Egr1 (NM_012551.2)	98	5′-CTACGAGCACCTGACCACAGAGTC-3′ (204–227)	5′-GCAACCGGGTAGTTTGGCT-3′ (283–301)
Gapdh (NM_017008.3)	93	5′-CCAAGGTCATCCATGACAACTT-3′ (476–497)	5′-AGGGGCCATCCACAGTCTT-3′ (550–568)
Ptgs2 (NM_017232.3)	90	5′-GAAGAACTTACAGGAGAGAAAGAAATGG-3′ (1393–1420)	5′-CAGCAGGGCGGGATACAGT-3′ (1464–1482)
Dusp1 (NM_053769.3)	62	5′-GCGCGCTCCACTCAAGTC-3′ (337–354)	5′-GGGCAGGAAGCCGAAAAC-3′ (381–398)
Dusp5 (NM_133578.1)	70	5′-CGACATTAGCTCCCACTTTCAA-3′ (882–903)	5′-AGGACCTTGCCTCCCTCTTC-3′ (934–953)
Areg (NM_017123.1)	108	5′-CTGCTGGTCTTAGGCTCAGG-3′ (218–237)	5′-CACAAGTCCACCAGCACTGT-3′ (306–325)
Il6 (NM_012589.1)	157	5′-GAGTTGTGCAATGGCAATTC-3′ (202–221)	5′-ACTCCAGAAGACCAGAGCAG-3′ (339–358)
Il1rl1 (NM_013037.1)	100	5′-GCCCTTCATCTGGGCTACACT-3′ (68–88)	5′-GCAATGGCACAGGAAGGTAAC-3′ (147–167)
(b) sqPCR primers			
Atf3 (NM_012912.1)	331	5′-GCTGCCAAGTGTCGAAACAAG-3′ (298–318)	5′-CAGTTTTCCAATGGCTTCAGG-3′ (608–628)
Gapdh (NM_017008.3)	452	5′-ACCACAGTCCATGCCATCAC-3′ (520–539)	5′-TCCACCACCCTGTTGCTGTA-3′ (952–971)

Table S3 Response of cardiomyocyte transcriptome to adenoviral infection

Cardiomyocytes were uninfected (no virus) or infected with empty AdVs and gene expression profiles were examined using Affymetrix microarrays. The data were analysed using GeneSpring to identify transcripts that were significantly changed (>1.5-fold, FDR < 0.05) by AdV infection. Transcripts are clustered according to known or probable function and are listed alphabetically with up-regulated transcripts listed first. Results are means for $n = 3$ independent hybridizations each representing three separate preparations of cardiomyocytes.

Probeset	Gene symbol	Gene description	Raw values (no virus)	Fold change induced by virus
(a) Antiviral response				
7196285	*Adar*	Adenosine deaminase, RNA-specific	204	1.80*
7315869	*Ddit3*	DNA-damage inducible transcript 3	273	2.27*
7301235	*Ifi27*	Interferon α-inducible protein 27	1785	1.98*
7072322	*Ifi35*	Interferon-induced protein 35	91	1.97*
7215722	*Ifi44*	Interferon-induced protein 44	126	3.96*
7067089	*Ifi47*	Interferon-inducible protein 47	141	7.07*
7041465	*Ifit2*	Interferon-induced protein with tetratricopeptide repeats 2	89	1.89*
7041467	*Ifit3*	Interferon-induced protein with tetratricopeptide repeats 3	57	3.38*
7170909	*Iigp1*	Interferon inducible GTPase 1	106	4.47*
7067595	*Irf1*	Interferon regulatory factor 1	154	1.72*
7131960	*Irf9*	Interferon regulatory factor 9	443	2.28*
7092176	*Mx1|2*	Myxovirus (influenza virus) resistance 1/2	55	19.37*
7087207	*Mx2|1*	Myxovirus (influenza virus) resistance 2/1	122	19.05*
7098547	*Oas1a/k*	2′-5′ Oligoadenylate synthetase 1A/K	91	12.05*
7102451	*Oas1b/i*	2′-5′ Oligoadenylate synthetase 1B/I	55	6.03*
7098544	*Oas1i*	2′-5′ Oligoadenylate synthetase 1I	73	5.81*
7102456	*Oas1k/a*	2′-5′ Oligoadenylate synthetase 1K/A	97	1.80*
7103432	*Oas2*	2′-5′ Oligoadenylate synthetase 2	41	3.58*
7102992	*Oasl*	2′-5′ Oligoadenylate synthetase-like	101	11.64*
7103001	*Oasl2*	2′-5′ Oligoadenylate synthetase-like 2	84	9.95*
7339147	*Plscr1*	Phospholipid scramblase 1	104	1.69*
7305174	*Rsad2*	Radical *S*-adenosylmethionine domain-containing 2	61	12.13*
7055354	*Trim5*	Tripartite motif-containing 5	835	1.52
7263822	*Zc3hav1*	Zinc finger CCCH type, antiviral 1	124	2.05
(b) Cytokine/chemokine signalling				
7073869	*C1qtnf1*	C1q and tumour necrosis factor-related protein 1	189	1.58
7356847	*Ccl20*	Chemokine (C-C motif) ligand 20	146	1.77
7070340	*Ccl7*	Chemokine (C-C motif) ligand 7	1918	2.00
7212626	*Csf1*	Colony-stimulating factor 1 (macrophage)	122	1.84
7071906	*Csf3*	Colony-stimulating factor 3 (granulocyte)	220	2.80
7116933	*Cxcl10*	Chemokine (C-X-C motif) ligand 10	37	5.21
7116931	*Cxcl11*	Chemokine (C-X-C motif) ligand 11	472	1.81
7123570	*Cxcl13*	Chemokine (C-X-C motif) ligand 13	132	1.69

Table S3 Continued

Probeset	Gene symbol	Gene description	Raw values (no virus)	Fold change induced by virus
7055111	*Il18bp*	IL18-binding protein	155	1.92
7260080	*Il6*	IL6	149	5.13
7138335	*Ripk3*	Receptor-interacting serine-threonine kinase 3	151	1.71
7362008	*Stat1/4*	Signal transducer and activator of transcription 1/4	906	2.26
7311784	*Stat2*	Signal transducer and activator of transcription 2	157	3.36
7216733	*Tnf*	Tumour necrosis factor (TNF superfamily, member 2)	94	2.19
7327525	*Tnfrsf11b*	Tumour necrosis factor receptor superfamily, member 11b	1001	1.93
7098502	*Trafd1*	TRAF (tumour-necrosis-factor-receptor-associated factor) type zinc finger domain containing 1	192	1.50
7351276	*Ccr1*	Chemokine (C-C motif) receptor 1	123	0.53
7041124	*Il33*	IL33	100	0.64
7123902	*Pf4*	Platelet factor 4	704	0.59
(c) Immune/inflammatory response				
7149693	*Bst2*	Bone marrow stromal cell antigen 2	165	3.21*
7093567	*Cd80*	CD80 molecule	80	2.20
7093779	*Cd86*	CD86 molecule	106	1.63
7216827	*Cfb*	Complement factor B	66	2.85
7296860	*Cmpk2*	Cytidine monophosphate (UMP-CMP) kinase 2, mitochondrial	72	7.20*
7327552	*Enpp2*	Ectonucleotide pyrophosphatase/phosphodiesterase 2	127	2.31
7107717	*Fcgr3a*	Fc fragment of IgG, low affinity IIIa, receptor	160	2.86
7200128	*Gbp2*	Guanylate-binding protein 2	101	7.94*
7076940	*Irgm*	Immunity-related GTPase family, M	240	6.43
7293880	*Isg15*	ISG15 ubiquitin-like modifier	64	14.88*
7033289	*Isg20*	Interferon-stimulated exonuclease gene 20	84	2.56*
7270067	*Klrk1*	Killer cell lectin-like receptor subfamily K, member 1	28	1.72
7084895	*Lgals3bp*	Lectin, galactoside-binding, soluble, 3 binding protein	319	3.79*
7080131	*Lgals5/9*	Lectin, galactose-binding, soluble 5/9	116	2.19*
7080134	*Lgals9/5*	Lectin, galactoside-binding, soluble, 9/5	162	4.47*
7069999	*Nos2*	Nitric oxide synthase 2, inducible	65	1.87
7266324	*Reg3g*	Regenerating islet-derived 3γ	1758	1.57
7216994		RT1 class Ia, locus A2/A1 | locus A3 | RT1 class Ib, locus EC2 | MHC class I RT1.Aa alpha-chain	289	2.02
7220575		RT1 class I, locus1 | RT1 class I, locus CE12/CE14	271	2.24
7216676		RT1 class I, locus CE10/CE7/CE11	164	1.72
7224452		RT1 class I, locus CE11/CE7 | RT1 class Ib, locus EC2	271	2.00
7224458		RT1 class I, locus CE12/14 | RT1 class I, locus1	244	2.31
7224429		RT1 class I, locus CE13/CE14	102	1.78
7224511		RT1 class I, locus CE15	422	1.76
7220557		RT1 class I, locus CE3/A3 | RT1 class Ia, locus A1/A2 | RT1 class Ib, locus EC2	116	1.75
7220541		RT1 class I, locus CE5/CE4 | RT1 class Ib, locus EC2 | MHC class I RT1.Aa alpha-chain | mature alpha chain of MHC class Ib protein-like	327	2.04
7216505		RT1 class Ib, locus N2/N1/N3	103	1.66
7216519		RT1 class Ib, locus N3/N1/N2	189	2.17
7216562		RT1 class I, locus T24, gene 1/4 | MHC class I RT1.O type 149 processed pseudogene	198	2.09
7216540		RT1 class I, locus T24, gene 1/1/4 | MHC class I | RT1.O type 149 processed pseudogene | RT1 class Ib, locus EC2	210	3.82
7220923	*Tap1*	Transporter 1, ATP-binding cassette, sub-family B (MDR/TAP)	120	3.12
7220903	*Tap2*	Transporter 2, ATP-binding cassette, sub-family B (MDR/TAP)	106	1.77
7221026	*Tapbp*	TAP-binding protein	239	2.78
7269637	*Tapbpl/Vamp1*	TAP-binding proteinlike | vesicle-associated membrane protein 1	113	1.59
7145662	*Tlr3*	Toll-like receptor 3	80	1.83
7226106	*Tor1b*	Torsin family 1, member B	154	1.51*
7112701	*Tor3a*	Torsin family 3, member A	162	1.91*
7071036	*Trim25*	Tripartite motif-containing 25	194	2.01*
7295338	*Xdh*	Xanthine dehydrogenase	155	1.56*
7226238	*Aif1l| Lamc3*	Allograft inflammatory factor 1-like | laminin γ3	920	0.65*
7111837	*Cfh*	Complement factor H	122	0.60
7325371	*Lyz2| Lyc2*	Lysozyme 2 | lysozyme C type 2	350	0.59
7321134	*Mir196a*	MicroRNA mir-196a	72	0.66*
(d) Agonists/receptors				
7035427	*Adm*	Adrenomedullin	210	1.52
7322881	*Angptl4*	Angiopoietin-like 4	186	1.74
7301401	*Bdkrb1*	Bradykinin receptor B1	53	1.81*
7232862	*Bmp2*	Bone morphogenetic protein 2	40	1.97
7123853	*Ereg*	Epiregulin	55	2.55
7204090	*Fst*	Follistatin	83	1.93
7144218	*Gdf15*	Growth differentiation factor 15	168	2.89

Table S3 Continued

Probeset	Gene symbol	Gene description	Raw values (no virus)	Fold change induced by virus
7261075	*Hgf*	Hepatocyte growth factor	155	1.57
7348035	*Htr1b*	5-hydroxytryptamine (serotonin) receptor 1B	33	1.60
7318105	*Ly6e*	Lymphocyte antigen 6 complex, locus E	127	2.89
7216279	*Olr1730*	Olfactory receptor 1730	42	1.64
7201157	*Ptger3*	Prostaglandin E receptor 3 (subtype EP3)	64	1.59
7055094	*Folr2*	Folate receptor 2 (fetal)	174	0.66
7364798	*Htr2b*	5-hydroxytryptamine (serotonin) receptor 2B	99	0.65
7313468	*Igf1*	Insulin-like growth factor 1	2690	0.36
7071991	*Igfbp4*	Insulin-like growth factor binding protein 4	494	0.63
7146031	*Msr1*	Macrophage scavenger receptor 1	640	0.57
7055209	*Olr63*	Olfactory receptor 63	180	0.61
7263730	*Ptn*	Pleiotrophin	825	0.37
7094158	*Tfrc*	Transferrin receptor	1300	0.58
(e) Cell adhesion/extracellular matrix				
7296103	*Sdc1*	Syndecan 1	184	1.78
7247754	*Sdc4*	Syndecan 4	1059	1.57
7213140	*Vcam1*	Vascular cell adhesion molecule	1140	1.78
7202072	*Vcan*	Versican	618	1.62
7317088	*Col14a1*	Collagen, type XIV, α1	271	0.64
7319496	*Fbln1*	Fibulin 1	299	0.65
7260805	*Fgl2*	Fibrinogen-like 2	254	0.60
7169581	*Pcdhb21*	Protocadherin β21	88	0.65
(f) Cell cycle/cell death				
7341999	*Birc3*	Baculoviral IAP repeat-containing 3	70	1.55
7321430	*Cdk2*	Cyclin-dependent kinase 2	229	1.57
7217282	*Cdkn1a*	Cyclin-dependent kinase inhibitor 1A	1072	2.49
7114725	*Ephx1*	Epoxide hydrolase 1, microsomal	124	2.25
7041442	*Fas*	Fas (tumour necrosis receptor superfamily member 6)	275	1.62
7055435	*Hpx*	Haemopexin	93	2.43
7325416	*Mdm2*	Mdm2 p53-binding protein homologue (mouse)	678	1.64
7211447	*Mllt11*	Myeloid/lymphoid or mixed-lineage leukaemia (trithorax homologue, *Drosophila*); translocated to, 11	121	1.62
7192589	*Tnfsf10*	Tumour necrosis factor (ligand) superfamily, member 10	53	2.00
7207681	*Ccna2*	Cyclin A2	261	0.56
7203074	*Ccnb1*	Cyclin B1	354	0.66
7218195	*Cdc2*	Cell division cycle 2, G_1 to S and G_2 to M	234	0.55
7132836	*Pbk*	PDZ-binding kinase	164	0.57
7338657	*Ttk*	Ttk protein kinase	88	0.64
(g) Protein synthesis/modification/folding/degradation				
7088621	*Dtx3l*	Deltex 3-like (*Drosophila*)	55	2.16
7114108	*Eef1g|Slamf7*	Eukaryotic translation elongation factor 1γ SLAM family member 7	302	1.56
7260038	*Mettl20*	Methyltransferase like 20	114	1.52
7361254	*Mitd1*	MIT, microtubule interacting and transport, domain containing 1236	2.46	
7220914	*Psmb8*	Proteasome (prosome, macropain) subunit, β type 8 (large multifunctional peptidase 7)	62	1.76
7216935	*Psmb9*	Proteasome (prosome, macropain) subunit, β type 9 (large multifunctional peptidase 2)	170	3.44
7138231	*Psme2*	Proteasome (prosome, macropain) activator subunit 2	1159	1.61
7103916	*Serpinb2*	Serine (or cysteine) peptidase inhibitor, clade B, member 2	180	7.32
7101220	*Serpine1*	Serine (or cysteine) peptidase inhibitor, clade E, member 1	214	1.98*
7241130	*Serping1*	Serine (or cysteine) peptidase inhibitor, clade G, member 1	597	1.55*
7195163	*Serpini1*	Serine (or cysteine) peptidase inhibitor, clade I, member 1	113	2.12
7247744	*Slpi|Slpil2*	Secretory leucocyte peptidase inhibitor|antileukoproteinase-like 2	1043	2.21
7374050	*Capn6*	Calpain 6	107	0.57
7332657	*Mmp12*	Matrix metallopeptidase 12	1365	0.44
(h) Regulation of metabolism/signalling/transcription				
7250403	*Abcb1b/1a*	ATP-binding cassette, sub-family B (MDR/TAP),member 1B/1A	175	3.24
7318515	*Apol3*	Apolipoprotein L, 3	168	1.53
7226167	*Ass1*	Argininosuccinate synthetase 1	216	1.85
7356120	*Cyp27a1*	Cytochrome P450, family 27, subfamily a, polypeptide 1	218	1.90
7352252	*Enpp4*	Ectonucleotide pyrophosphatase/phosphodiesterase 4	243	1.72
7363922	*Glb1l*	Galactosidase, β1-like	150	1.54
7327675	*Has2*	Hyaluronan synthase 2	256	1.78
7037881	*Mgmt*	*O*-6-methylguanine-DNA methyltransferase	158	1.54
7185182	*Nqo1*	NAD(P)H dehydrogenase, quinone 1	241	1.52
7093806	*Parp9*	Poly (ADP-ribose) polymerase family, member 9	80	1.81
7329573	*Pvalb*	Parvalbumin	57	1.56
7237508	*Ptges*	Prostaglandin E synthase	252	3.02
7106132	*Ptgs2*	Prostaglandin-endoperoxide synthase 2	136	1.92
7339559	*Rbp2*	Retinol-binding protein 2, cellular	93	2.28

Table S3 Continued

Probeset	Gene symbol	Gene description	Raw values (no virus)	Fold change induced by virus
7041029	*Rcl1*	RNA terminal phosphate cyclase-like 1	391	1.57
7244077	*Slc28a2*	Solute carrier family 28 (sodium-coupled nucleoside transporter), member 2	174	1.57
7250503	*Steap1*	Six transmembrane epithelial antigen of the prostate 1	419	1.81
7184185	*Asf1b*	ASF1 anti-silencing function 1 homologue B (*S. cerevisiae*)	176	0.65
7115455	*Atf3*	Activating transcription factor 3	183	0.45
7197511	*Casq2*	Calsequestrin 2 (cardiac muscle)	1048	0.58
7156835	*F13a1*	Coagulation factor XIII, A1 polypeptide	237	0.34
7250763	*Gng11*	Guanine nucleotide-binding protein (G protein), gamma 11	826	0.65
7164749	*Hist1h2ail*	Histone cluster 1, H2ai-like	1978	0.62
7034549	*Kcne3*	Potassium voltage-gated channel, Isk-related subfamily, gene 3	548	0.61
7240783	*Pde1a*	Phosphodiesterase 1A, calmodulin-dependent	343	0.61
7261911	*Pdk4*	Pyruvate dehydrogenase kinase, isozyme 4	219	0.66
7288397	*Ptplad2*	Protein tyrosine phosphatase-like A domain containing 2	141	0.66
7362066	*Sdpr*	Serum deprivation response	835	0.56
7219202	*Smpdl3a*	Sphingomyelin phosphodiesterase, acid-like 3A	618	0.65
7025936	*Tcf21*	Transcription factor 21	724	0.63
(i) Proteins with no known function/hypothetical proteins				
7329479	*Apol9a*	Apolipoprotein L 9a	147	4.07
7220127	*Ascc3*	Activating signal cointegrator 1 complex subunit 3	215	1.77
7070512	*LOC360228*	WDNM1 homologue	139	1.57
7333434	*LOC500956*	Unknown	150	1.53
7138718	*Phf11/11l*	PHD finger protein 11/11-like	46	2.81
7260055	*RGD1309621*	Similar to hypothetical protein FLJ10652	155	2.46
7065377	*RGD1561157*	Unknown	117	1.71
7235527	*Rnf114*	Ring finger protein 114	951	1.70*
7073915	*Rnf213*	Ring finger protein 213	51	2.54
7073928	*Rnf213*	Ring finger protein 213	65	1.99
7094771	*Rtp4|Ctdsp1*	Receptor (chemosensory) transporter protein 4 | CTD (carboxy-terminal domain, RNA polymerase II, polypeptide A) small phosphatase 1	139	11.46*
7070419	*Slfn3*	Schlafen 3	131	5.04*
7070393	*Slfn5*	Schlafen family member 5	98	1.85*
7072336	*Tmem106a*	Transmembrane protein 106A	78	1.85
7252491	*Tmem140*	Transmembrane protein 140	206	1.83
7047575	Unknown	Unknown	55	1.57
7088625	Unknown	Unknown	88	2.72
7116103	Unknown	Unknown	71	2.16
7129836	Unknown	Unknown	38	1.54
7153410	Unknown	Unknown	96	1.74
7254427	Unknown	Unknown	119	1.55
7328454	Unknown	Unknown	46	1.64
7371101	Unknown	Unknown	54	2.67
7126637	*Cd38*	CD38 molecule	608	0.61
7191192	*Fam134b*	Family with sequence similarity 134, member B	1202	0.62
7372873	*Fam70a*	Family with sequence similarity 70, member A	534	0.51
7133474	*Lcp1*	Lymphocyte cytosolic protein 1	545	0.57
7164764	*LOC680097*	Similar to germinal histone H4 gene	6612	0.58
7367891	*LOC680166*	Unknown	204	0.61
7157871	*LOC682649*	Similar to Histone H2A type 1	647	0.53
7260779	*Lrrc17*	Leucine rich repeat containing 17	298	0.38
7060488	*Ms4a6b/11*	Membrane-spanning 4-domains, subfamily A, member 6B/11	215	0.52
7337370	*Ns5atp9*	NS5A (hepatitis C virus) transactivated protein 9	307	0.66
7035206	*Olfml1*	Olfactomedin-like 1	355	0.48
7328472	*Tmem71*	Transmembrane protein 71	128	0.59
7077262	Unknown	Unknown	100	0.66
7135004	Unknown	Unknown	194	0.62
7164849	Unknown	Unknown	845	0.66
7176278	Unknown	Unknown	208	0.65
7367340	Unknown	Unknown	67	0.57
7368283	Unknown	Unknown	409	0.63
7369003	Unknown	Unknown	1284	0.63
7370879	Unknown	Unknown	86	0.63

*Transcripts identified as part of an interferon response in other systems.

Table S4 Transcripts up-regulated by ET-1 that are regulated by Atf3, but are unaffected by No-AS virus infection

*IEG; **non-IEG.

			Control			ET-1		
Transcript cluster	Gene symbol	Raw values	No virus	No-AS	AS-Atf3	No virus	No-AS	AS-Atf3
(a) AS Atf3 enhances response to ET-1								
Cluster A1								
7169197	*Egr1**	289	1	0.95	1.02	1.29	1.24	4.73
7222466	*Egr2**	85	1	0.92	0.87	1.32	1.59	2.90
7288744	*Jun**	425	1	0.93	1.44	1.21	1.31	2.10
7320920	*Nr4a1**	64	1	0.95	1.12	3.78	4.29	6.63
Cluster A2								
7308330	*Actn1**	152	1	0.94	2.61	2.72	2.22	3.56
7185572	*Bcar1**	154	1	1.05	1.94	1.56	1.41	2.23
7231595	*Chac1***	142	1	1.01	2.04	0.96	1.08	3.03
7114850	*Enah**	130	1	0.98	2.28	2.00	1.60	2.86
7265600	*Gadd45a***	854	1	1.00	2.94	1.98	1.93	3.09
7243216	*Grem1***	52	1	1.13	1.81	1.83	1.49	2.68
7179800	*Ier2**	368	1	0.96	2.16	1.67	1.79	4.56
7354973	*Nop58*	195	1	0.95	2.86	1.93	1.62	3.39
7124933	*Rasl11b**	500	1	1.13	2.22	1.73	1.91	3.02
7096358	*Slc7a1***	88	1	1.10	2.80	2.18	1.74	3.54
7115195	*Tgfb2***	181	1	1.06	2.77	1.79	1.67	2.99
(b) AS Atf3 inhibits response to ET-1								
Cluster B1								
7260283	*Insig1*	2796	1	0.94	0.62	1.54	1.50	0.95
7144691	*Sc4mol***	1376	1	0.99	0.60	1.72	1.72	0.89
7133039	*Stc1**	560	1	1.17	0.58	1.21	1.23	0.59
Cluster B2								
7123129	*Agpat9*	65	1	0.96	1.07	2.82	2.22	1.40
7123848	*Areg***	127	1	1.07	1.20	5.63	7.01	2.09
7043230	*Dusp5***	178	1	0.93	0.87	3.03	2.99	1.54
7345585	*Fdx1***	459	1	0.87	0.93	2.94	3.05	1.98
7187674	*Glrx1*	191	1	0.94	0.82	1.66	1.92	1.14
7202670	*Hmgcr**	527	1	1.00	0.72	1.62	1.71	1.04
7150663	*Mfap3l*	116	1	0.98	0.91	1.66	1.34	0.88
7235566	*Pard6b***	62	1	1.06	1.19	3.20	3.62	1.48
7204067	*Pelo***	863	1	1.12	1.19	1.76	1.90	1.24
7104906	*RGD1562617*	127	1	0.90	0.88	2.36	1.41	0.89
7214260	*Sgms2*	77	1	1.03	1.04	4.42	3.27	1.28
7141508	*Spry2***	513	1	0.99	1.20	2.87	2.79	1.74
7297329	*Twist1***	126	1	1.14	0.96	2.83	3.77	2.24
7350922	*Xirp1***	217	1	1.02	1.40	4.09	3.53	1.70
7297247	Unknown	121	1	1.12	1.14	2.21	2.22	1.41

Table S5 Transcripts unaffected by No-AS virus infection that are up-regulated by ET-1 with significantly increased expression in control cells by Atf3 knockdown

*IEG; **non-IEG.

			Control			ET-1		
Transcript cluster	Gene symbol	Raw values	No virus	No-AS	AS-Atf3	No virus	No-AS	AS-Atf3
Cluster C								
7305953	*Arl4a*	482	1	1.07	1.69	1.60	1.99	1.61
7301400	*Bdkrb2***	104	1	1.09	1.77	1.74	1.98	2.21
7111272	*Btg2**	311	1	0.93	1.87	3.66	4.22	3.28
7209338	*Ccnl1**	249	1	0.99	1.77	1.69	1.54	2.47
7045969	*Cnksr3*	166	1	1.14	1.96	1.61	1.63	2.21
7350918	*Csrnp1*	146	1	1.17	2.42	3.63	3.82	4.59
7044959	*Ctgf**	342	1	0.91	3.04	3.85	4.13	5.22
7215359	*Cyr61**	407	1	1.04	1.74	5.22	5.40	6.22
7143265	*Eaf1*	130	1	1.13	1.87	1.56	1.57	2.12
7163221	*Edn1**	71	1	1.11	1.78	1.19	1.26	2.42
7147985	*Efnb2***	71	1	0.99	1.74	1.42	1.45	2.15
7281135	*Epha2**	90	1	1.16	3.52	2.89	3.29	4.32
7297136	*Fam110c*	55	1	1.09	1.92	3.70	4.75	3.76
7242382	*Fjx1*	149	1	1.07	1.74	1.74	1.71	2.10
7252051	*Flnc***	143	1	0.94	1.47	2.86	2.31	1.80
7162363	*Gadd45g**	357	1	0.99	3.33	4.72	4.19	5.92
7174562	*Hbegf**	100	1	0.88	2.73	3.90	4.33	3.84
7193413	*Hspa4l*	63	1	0.93	2.29	1.94	1.48	2.00
7165193	*Inhba***	88	1	1.09	2.09	6.95	6.30	6.29
7257290	*Lmcd1**	283	1	1.17	4.41	5.84	6.64	5.84
7100653	*Mafk**	187	1	1.00	2.06	2.23	2.25	2.36
7068314	*Map2k3***	106	1	1.00	1.65	1.91	1.78	1.96
7194351	*Mei1/Tsc22d2*	149	1	0.99	1.84	2.45	2.43	2.43
7317471	*Myc**	156	1	1.02	2.04	2.28	2.34	2.92
7155813	*Nfil3**	67	1	1.04	2.71	2.57	2.83	3.71
7189518	*Plk2**	1457	1	1.15	2.79	2.14	2.65	3.58
7051029	*Ppp1r15a*	115	1	1.02	1.93	1.57	1.57	2.26
7360736	*Ptp4a1*	638	1	1.05	2.14	2.39	2.27	2.36
7048738	*PVR**	430	1	1.16	2.58	3.64	3.77	3.48
7340175	*Rassf1**	163	1	0.99	1.90	1.62	1.68	2.04
7091811	*Rcan1*	2101	1	1.12	1.77	1.90	1.95	1.95
7331581	*Rnd1**	203	1	1.20	3.24	4.78	4.76	3.58
7238766	*Rnd3**	311	1	1.01	1.96	1.82	1.56	2.00
7029999	*Sertad1**	217	1	1.09	1.86	1.95	2.50	2.39
7279509	*Stk40*	144	1	1.00	1.64	1.62	1.57	1.75
7075088	*Tnfrsf12a**	750	1	1.09	2.75	3.17	3.26	3.77
7106964	*Tnfsf18*	80	1	0.87	2.02	9.32	6.92	9.29
7199859	*Tspan5***	217	1	1.08	1.69	2.30	2.02	1.95
7120783	Unknown	93	1	0.92	1.47	1.64	1.52	1.55
7339862	Unknown	185	1	0.84	1.53	1.62	1.14	1.60
7085544	*Vgll3*	133	1	0.96	1.59	2.87	2.52	2.78
7228236	*Xirp2*	124	1	0.93	2.14	3.84	2.73	2.17

Table S6 Transcripts affected by No-AS virus infection that are up-regulated by ET-1 and regulated by Atf3

*IEG; **non-IEG.

			Control			ET-1		
Transcript cluster	Gene symbol	Raw values	No virus	No-AS	AS-Atf3	No virus	No-AS	AS-Atf3
(a) AS-Atf3 enhances response to ET-1								
Cluster D								
7120521	*Lif**	82	1	1.75	3.70	2.88	3.62	7.30
7106132	*Ptgs2**	136	1	1.92	3.93	4.94	4.44	9.84
7237652	*Slc25a25**	94	1	1.22	1.71	1.41	1.64	2.19
7028549	*Il11*	143	1	1.20	1.74	2.88	2.82	3.87
7284153	*Ripk2***	238	1	1.31	2.79	2.53	2.72	3.58
7261019	*Sema3c*	208	1	1.22	2.16	1.67	1.80	2.21
7035407	*Wee1*	303	1	1.21	1.89	1.74	2.23	2.26
7096947	*Zfand2a**	288	1	1.23	1.60	1.73	2.17	2.39
(b) AS-Atf3 inhibits response to ET-1								
Cluster E								
7259100	*Apold1*	533	1	0.82	0.63	1.64	1.43	1.02
7105894	*B3galt2*	505	1	0.79	1.12	2.31	1.97	1.07
7051386	*Csrp3*	1062	1	0.75	0.72	1.53	1.37	0.72
7084788	*Socs3*	229	1	1.25	1.01	1.75	1.64	0.77
7370997	Unknown	313	1	0.69	0.81	1.83	1.43	0.80
7135004	Unknown	194	1	0.62	1.24	2.47	2.47	1.40
7305661	Unknown	81	1	0.80	1.25	3.46	3.56	2.12

Table S7 Transcripts that are down-regulated by ET-1 and regulated by Atf3

			Control			ET-1		
Transcript cluster	Gene symbol	Raw values	No virus	No-AS	AS-Atf3	No virus	No-AS	AS-Atf3
(a) AS-Atf3 enhances response to ET-1								
Cluster F								
7279127	*Cited4*	231	1	0.91	0.48	0.52	0.59	0.47
7180333	*Ednra*	2175	1	0.99	0.60	0.58	0.64	0.41
7115625	*G0s2*	2545	1	0.86	0.49	0.30	0.26	0.12
7190436	*Lifr*	390	1	0.88	0.55	0.60	0.54	0.37
7269707	*Ntf3*	250	1	1.18	0.54	0.52	0.65	0.37
(b) AS-Atf3 inhibits response to ET-1								
Cluster G								
7222734	*Ddit4*	1553	1	1.16	2.04	0.46	0.55	0.79
7120384	*Pik3ip1*	339	1	0.83	0.57	0.29	0.34	0.46
7346730	*Smad6*	266	1	1.05	1.41	0.50	0.57	1.03
7197113	*Txnip*	2024	1	0.90	1.10	0.32	0.39	0.96
7173133	Unknown	690	1	0.74	0.15	0.23	0.16	0.18

REFERENCES

1 Ben-Ari, Y., Brody, Y., Kinor, N., Mor, A., Tsukamoto, T., Spector, D. L., Singer, R. H. and Shav-Tal, Y. (2010) The life of an mRNA in space and time. J. Cell Sci. **123**, 1761–1774

2 Burkhard, K. A., Chen, F. and Shapiro, P. (2011) Quantitative analysis of ERK2 interactions with substrate proteins: roles for kinase docking domains and activity in determining binding affinity. J. Biol. Chem. **286**, 2477–2485

3 Cerbai, E., Pino, R., Sartiani, L. and Mugelli, A. (1999) Influence of postnatal-development on I_f occurrence and properties in neonatal rat ventricular myocytes. Cardiovasc. Res. **42**, 416–423

4 Fujioka, A., Terai, K., Itoh, R. E., Aoki, K., Nakamura, T., Kuroda, S., Nishida, E. and Matsuda, M. (2006) Dynamics of the Ras/ERK MAPK cascade as monitored by fluorescent probes. J. Biol. Chem. **281**, 8917–8926

5 Maiuri, P., Knezevich, A., De Marco, A., Mazza, D., Kula, A., McNally, J. G. and Marcello, A. (2011) Fast transcription rates of RNA polymerase II in human cells. EMBO Rep. **12**, 1280–1285

6 Murray, J. D. (1993) Mathematical Biology, Springer Verlag, New York

7 Qin, X., Ahn, S., Speed, T. P. and Rubin, G. M. (2007) Global analyses of mRNA translational control during early *Drosophila* embryogenesis. Genome Biol. **8**, R63

8 Satoh, H., Delbridge, L. M., Blatter, L. A. and Bers, D. M. (1996) Surface:volume relationship in cardiac myocytes studied with confocal microscopy and membrane capacitance measurements: species-dependence and developmental effects. Biophys. J. **70**, 1494–1504

9 Sugden, P. H., Markou, T., Fuller, S. J., Tham, E. L., Molkentin, J. D., Paterson, H. F. and Clerk, A. (2011) Monophosphothreonyl extracellular signal-regulated kinases 1 and 2 (ERK1/2) are formed endogenously in intact cardiac myocytes and are enzymically active. Cell. Signalling 23 468–477

10 Tinoco, Jr, I. and Wen, J. D. (2009) Simulation and analysis of single-ribosome translation. Phys. Biol. **6**, 025006

11 Vassilenko, K. S., Alekhina, O. M., Dmitriev, S. E., Shatsky, I. N. and Spirin, A. S. (2011) Unidirectional constant rate motion of the ribosomal scanning particle during eukaryotic translation initiation. Nucleic Acids Res. **39**, 5555–5567

12 Wohlgemuth, I., Pohl, C. and Rodnina, M. V. (2010) Optimization of speed and accuracy of decoding in translation. EMBO J. **29**, 3701–3709

Received 19 January 2012/29 February 2012; accepted 5 March 2012
Published as BJ Immediate Publication 5 March 2012, doi:10.1042/BJ20120125